AD NUMBER

AD805554

NEW LIMITATION CHANGE

TO

Approved for public release, distribution unlimited

FROM

Distribution authorized to U.S. Gov't. agencies and their contractors; Administrative/Operational Use; DEC 1966. Other requests shall be referred to Ballistic Systems Div., AFSC, Norton AFB, CA.

AUTHORITY

SAMSO USAF ltr, 28 Feb 1972

A SUMMARY ANALYSIS OF LABORATORY HYPERSONIC WAKE TRANSITION EXPERIMENTS

A. Goldburg

RESEARCH NOTE 672
December 1966

supported jointly by

BALLISTIC SYSTEMS DIVISION
DEPUTY FOR BALLISTIC MISSILE RE-ENTRY SYSTEMS
AIR FORCE SYSTEMS COMMAND
Norton Air Force Base, California
under Contract AF 04(694)-690

ADVANCED RESEARCH PROJECTS AGENCY
monitored by the
ARMY MISSILE COMMAND
UNITED STATES ARMY
Redstone Arsenal, Alabama
under Contract DA-01-021-AMC-12005(Z)
(part of Project DEFENDER)

AVCO EVERETT RESEARCH LABORATORY
A DIVISION OF AVCO CORPORATION

BSD-TR-66-375 RESEARCH NOTE 672

A SUMMARY ANALYSIS OF LABORATORY HYPERSONIC WAKE TRANSITION EXPERIMENTS

by

A. Goldburg

AVCO EVERETT RESEARCH LABORATORY
a division of
AVCO CORPORATION
Everett, Massachusetts

December 1966

supported jointly by

BALLISTIC SYSTEMS DIVISION
DEPUTY FOR BALLISTIC MISSILE RE-ENTRY SYSTEMS
AIR FORCE SYSTEMS COMMAND
Norton Air Force Base, California

under Contract AF 04(694)-690

ADVANCED RESEARCH PROJECTS AGENCY
monitored by the
ARMY MISSILE COMMAND
UNITED STATES ARMY
Redstone Arsenal, Alabama

under Contract DA-01-021-AMC-12005 (Z)
(part of Project DEFENDER)

FOREWORD

This report has been supported jointly by Avco Everett Research Laboratory under Contract AF 04(694)-690 for Ballistic Systems Division, Deputy for Ballistic Missile Re-entry Systems, Air Force Systems Command, Norton Air Force Base, California, and Advanced Research Projects Agency, monitored by the Army Missile Command, United States Army, Redstone Arsenal, Alabama under Contract DA-01-021-AMC-12005 (Z) (part of Project DEFENDER). The secondary report number as assigned by AERL is Avco Everett Research Laboratory Research Note 672. The Air Force program monitor for contract AF 04(694)-690 is Thomas W. Swartz, 1st Lt., USAF, Project Officer.

Publication of this report does not constitute Air Force approval of the report's findings or conclusions. It is published only for the exchange and stimulation of ideas.

Thomas W. Swartz, 1st Lt.
USAF, Project Officer

ABSTRACT*

Hypersonic Wake Transition data over a range of Reynolds numbers have been obtained over the past several years at many laboratories. In the present paper, the available experimental data is structured into three laws: The Law of the Far Wake, The Law of the Near Wake, and The Law of the Interpolation Regime. These three laws are then represented on a single Hypersonic Wake Transition Map.

The Reynolds number is selected as the correlating parameter, where local conditions, characterizing the state of the gas at transition are used for the property values. The correlating constant is determined from the ballistic range data. For high Mach number flows, binary scaling allows the representation of the Reynolds number as a pressure times a length.

In the Far Wake, for the first onset of wake unsteadiness, the wake velocity profiles have reached their asymptotic behavior, density gradients have become small, and details of body shape have been lost. For this region, the characteristic length is represented as $\sqrt{C_D A}$ based on the total drag of the body. The Far Wake transition rule becomes $p_\infty \cdot \sqrt{C_D A} = \text{constant}$.

In the Near Wake, local hypersonic phenomena depending on body shape dominate the flow field. Here the characteristic length is the distance from the wake origin to the onset of unsteadiness, x_{tr}. As in boundary layer flow this correlation shows a strong dependence on an appropriate local Mach number, M_e, at the point of wake transition: $p_\infty \cdot x_{tr} = \text{constant}$, a function of M_e.

In the Interpolation Regime, one traverses from the Near to the Far Wake. The strong favorable pressure gradient, the strong density gradients and the effect of body shape becomes less important as one proceeds downstream along the Wake in the Interpolation regime. Thus, ideas derived from the Navier-Stokes equation are useful and lead with the aid of the ballistic range data to a sufficiently accurate general interpolation curve to connect the Far Wake Law with the Near Wake Law. The Interpolation curve, like the $p_\infty \cdot \sqrt{C_D A}$ Far Wake and the $p_\infty \cdot x_{tr}$ Near Wake correlations is good to a factor of 2 in the pressure.

The Transition Map provides a method for making the transition curve, x_{tr} as function of pressure ratio (altitude), for a given body at a given flight velocity: Connect the Far Wake onset altitude for the $\sqrt{C_D A}$ of the body with the Near Wake $Re_{x_{tr}}$ behavior for the corresponding M_{sh} of the body. Thus a complete qualitative Wake Transition Map is presented for a large range of Mach numbers and body sizes and body shapes.

*This paper is a summary of the author's work on this topic over the several years he was associated with Avco Everett Research Laboratory. It is being published at this time for the purpose of exchange and stimulation of ideas and not as an implicit approval of the findings and conclusions therein.

TABLE OF CONTENTS

LIST OF SYMBOLS

a	speed of sound
A	projected area of body
C_D	total drag coefficient
C_M	constant in Near Wake correlation, a function of M_{sh}
d	projected body diameter
ℓ	length of the body
M	Mach number
$\bar{M}_{es}$	defined in Equation 3
p_∞	free stream pressure
P	p_∞ divided by sea level pressure
R	Reynolds number; unless otherwise stated, taken at the body shoulder as being sufficiently representative of local wake flow conditions
R_{cr}	minimum Reynolds number for amplification of small disturbances
u	mean flow velocity parallel to the center line of the flow field
U_∞	free stream velocity
x	downstream position relative to base of body
y	coordinate normal to center line of flow field
ρ_∞	free stream density
θ	wake momentum thickness based on total drag

Subscripts

ℓ	center line of flow field
e	external edge of shear layer

s	given spectral distribution
sh	shoulder values
sl	sea level
tr	transition value for x
T	transition value for R based on $\sqrt{C_D A}$

1. INTRODUCTION*

The intent of the present paper is to provide a rational framework for hypersonic wake transition which has a solid foundation in fluid mechanical concepts and understanding, into which valid transition information can be logically placed, and which will be usefully structured for the technological needs which motivate the problem.

The wakes behind hypervelocity bodies during atmospheric reentry and ballistic range flight can be observed by means of active (radar) or passive (self-luminous) electromagnetic radiation. The patterns of observables in the hypersonic wake may be thought of as being produced in the following way: Physical chemistry determines the observable tracers and fluid mechanics determines the mixing patterns. These two effects are formally related through the coupling between the fluid mechanical equations of motion (continuity and momentum); the equations related to the constituents of the fluid (species conservation); and the equations related to the constituents' quantum mechanical properties (energy); and the equation of state. The radiating and scattering properties of the gas are strongly influenced by the fluid mechanical mixing process which in turn is strongly affected by whether the mixing is being accomplished solely through molecular diffusion or whether, in addition, there is macroscopic mass interchange.

In order to recover the body description from the wake, information available in the wake must be extracted and used. The wake is a highly diffusive region. In diffusion processes, information is lost as time passes. In contradistinction to the wave equation, time in the diffusion equation proceeds in only one direction. Hence, the attempt to reconstruct the details of body mass and shape may require attention to the local distributions of wake properties.

The requirement to describe local property distributions in fluid mechanical flow fields introduces new questions for aerodynamicists. In the past, aerodynamics has been concerned with predicting time-averaged and space-averaged forces and heat transfer at solid surfaces.

---

*This report represents a summary of the author's work in the area of hypersonic wake transition over the several years he was associated with the Avco Everett Research Laboratory. Publication of this report does not constitute Avco Everett Research Laboratory's approval of the findings and conclusions therein. It is being published only for the exchange and stimulation of ideas.

Fortunately, one could be quite wrong about the local property distributions and yet obtain very useful answers for surface viscous effects.

Now, however, the requirement is for a description, local in space and local in time, of property distributions of interest - , e. g. , a velocity or a particular species concentration - as a function of reentry conditions. Further, if the flow is time dependent, a description of the local spectral distribution of the fluctuations of each important wake property may be required. In the case of radar scattering by the ionized turbulent hypersonic flow field, acting as a collection of single scatterers, the spatial correlation function of the refractive index fluctuations is required. Further, the scattering is determined by a narrow portion of the spectrum around ($\underset{\sim}{k} - k\left|\frac{\underset{\sim}{r}}{r}\right|$), where k is the wave number and $\underset{\sim}{r}$ the vector from the iliuminating source;* and hence, its prediction is sensitive to the accuracy with which such spectral distributions are described.

Past aerodynamic transition problems have been concerned with body related shear layers - either along or immediately separated from the surface boundary. In such body-related shear layers, the hypersonic transition process from laminar to small scale turbulence is compressed into a small distance relative to surface length of interest (say an airfoil chord length) due to the continuous generation of vortical energy along the surface. The past technological requirement for only space and time-averaged surface information and the narrowness of the transition region relative to the surface extent led to the concept of, "$x_{transition}$." It was "x_{tr}" that the forces or heat transfer went from the laminar value to the more or less turbulent value.

Transition in the hypersonic wake is more gradual since the vortical energy is created near the body alone and diffuses away as it passes downstream. Further, what is required for a description of electromagnetic scattering (and to a lesser extend for the prediction of self-luminous radiation) is the description in local space of the distributions of the time dependent properties in the frequency domain and their behavior with free stream conditions.

*Tatarski, V.I., Wave Propagation in a Turbulent Medium, McGraw-Hill, 1961.

2. THE PHENOMENOLOGY OF WAKE TRANSITION

The question of stability of flows to small perturbations is not the question of transition. However, the inherent instability of laminar motion at sufficiently high Reynolds numbers, R, is responsible for the ultimate transition to turbulent flow. The value of the transition Reynolds number, depends not only on the minimum critical Reynolds number, R_{cr}, determined from stability theory for infinitesimal disturbances, but also on the initial size of the actual disturbances with the most "dangerous" frequencies.

The approach adopted here to the problem of the inherent instability of steady fluid dynamic flows and the onset of turbulence is the classical one.[1] Conceptually, if small perturbations which inevitably occur in the flow tend to increase with time, then the flow is absolutely unstable. The absolute instability of the flow for $R > R_{cr}$ leads to the appearance of a nonsteady flow with characteristic period and with small but finite amplitude which increases with R. This periodic flow usually can be described in terms of a succession of vortex filaments. When the Reynolds number increases further, a time comes when the periodic flow in turn becomes unstable with the appearance of a new period. When the Reynolds number increases still further, more and more new periods appear in succession. The range of Reynolds numbers between successive appearances of new frequencies diminishes rapidly in size; the new flows themselves are on a smaller and smaller scale. The flow rapidly becomes complicated and confused and we say that such a flow is turbulent.

Consider steady wake flow in the x-direction. A slight perturbation whose wave components in the course of time are amplified is carried downstream. The energy in the velocity fluctuations builds up in the amplification regime into the ordered time dependent vortex flow with characteristic frequencies. Over a small range of Reynolds numbers this vortex system may persist to infinity, decaying through molecular diffusion alone. With subsequent increase in R, two things happen: (1) The effective origin – the downstream position at which there is a

certain level of energy density at the ordered frequency (and its harmonics) - of the vortex system moves upstream towards the body.[2]
(2) The velocity fluctuation wake energy in the ordered flow is continually passed down, with increasing distance downstream, to the energy in the random small scale eddy velocity fluctuations containing all frequencies. Finally, as $R \to \infty$, the boundary layer on the body is fully turbulent and the distribution of fluctuation energy density in the base region already has finite values at all frequencies.

In a comprehensive set of experiments at low speeds (rearward facing step,[3] rectangular jet,[4] and flat-plate wake,[5]) Sato has shown that transition in a free shear layer essentially follows the hierarchy described above: initiation by Tollmein waves that grow exponentially in the downstream direction, followed by a nonlinear regime characterised by a double row of vortices, and finally a region in which the fluctuation loses regularity and gradually develops into turbulence.

Leonard and Keck's modification of the conventional schlieren system uses a sodium vapor in the test medium with an interference filter in the optical domain with peak transmission 20 Å off the 5896 Å sodium line.[6] The extremely large value of the index of refraction at the resonance line greatly enhances the effective index of the test medium for the light passing through the filter. At the specified conditions, it is at least two orders of magnitude larger than that for air in the optical domain. This makes it possible to extend the pressure regime for good schlieren contrast from that of a few percent of atmospheric to pressures less than half of one percent, and to considerably increase the detail apparent in pictures taken in the two to three percent atmospheric region. Further, using a constant partial pressure of sodium vapor, the sensitivity of the schlieren system is constant and thus independent of the gas pressure.

Sodium schlieren pictures[6] allow the observation of the development of structure in the hypersonic sphere wake at the onset of transition. It is hypothesized that qualitatively the development is similar to the classical one described above. Near the body, small perturbations in the flow are in the form of Tollmien-Schlichting-like waves which, in

the course of time, are amplified and carried downstream. These waves are longitudinal in orientation and of several body diameters in length. The fluctuating wake energy builds up in the succeeding nonlinear amplification regime, and this growth process leads into a nearly ordered flow at a set of characteristic frequencies. This structure might be described as a succession of vortex filaments, which in the sphere case is like a procession of vortex loops, one tied to another.[7,8] Proceeding downstream, there is a continual degradation of the fluctuating wake energy from the nearly ordered nonsteady flow, with significant energy at distinct frequencies, down into random small scale fluctuations containing all frequencies and proceeding towards fully developed turbulence.

Figure 1 is a composite of five separate sodium schlieren pictures, each single picture taken on a separate run. All runs were made at constant fixed range pressure of 1.7 cm Hg of N_2. For the body size used in these experiments, d = 0.56 cm, this pressure is in the range of the onset of hypersonic wake transition to nonsteady flow.[8] Approximately 0.375 mm Hg partial pressure of sodium vapor was maintained in the test section. The pellet velocities varied experimentally by about plus or minus 10 percent from the mean of 14,000 ft/sec. (Hypersonic wake transition has been shown to be insensitive to 10 percent changes in velocity.[8,9]) The spark source was triggered by a variable time delay after the passage of the projectile, thus providing observations of various portions of the wake as shown. The knife edge was horizontal, thus emphasizing vertical gradients.

The photographs in Fig. 1 illustrate the hierarchy of transition modes. Horizontal wave-like striations of several body lengths long are plainly visible originating near to or from the base region. These correspond to the small perturbations mentioned above. The second picture shows these perturbations after some fluid mechanical amplifications. The striations are now formed into a nearly ordered flow and the structure appears to be like a procession of vortex filaments having loop-like shape. Weak shocks are visible emanating from some of these filaments, indicating their large scale and their large velocity relative to the inviscid flow. In the third photograph, the original perturbations have been

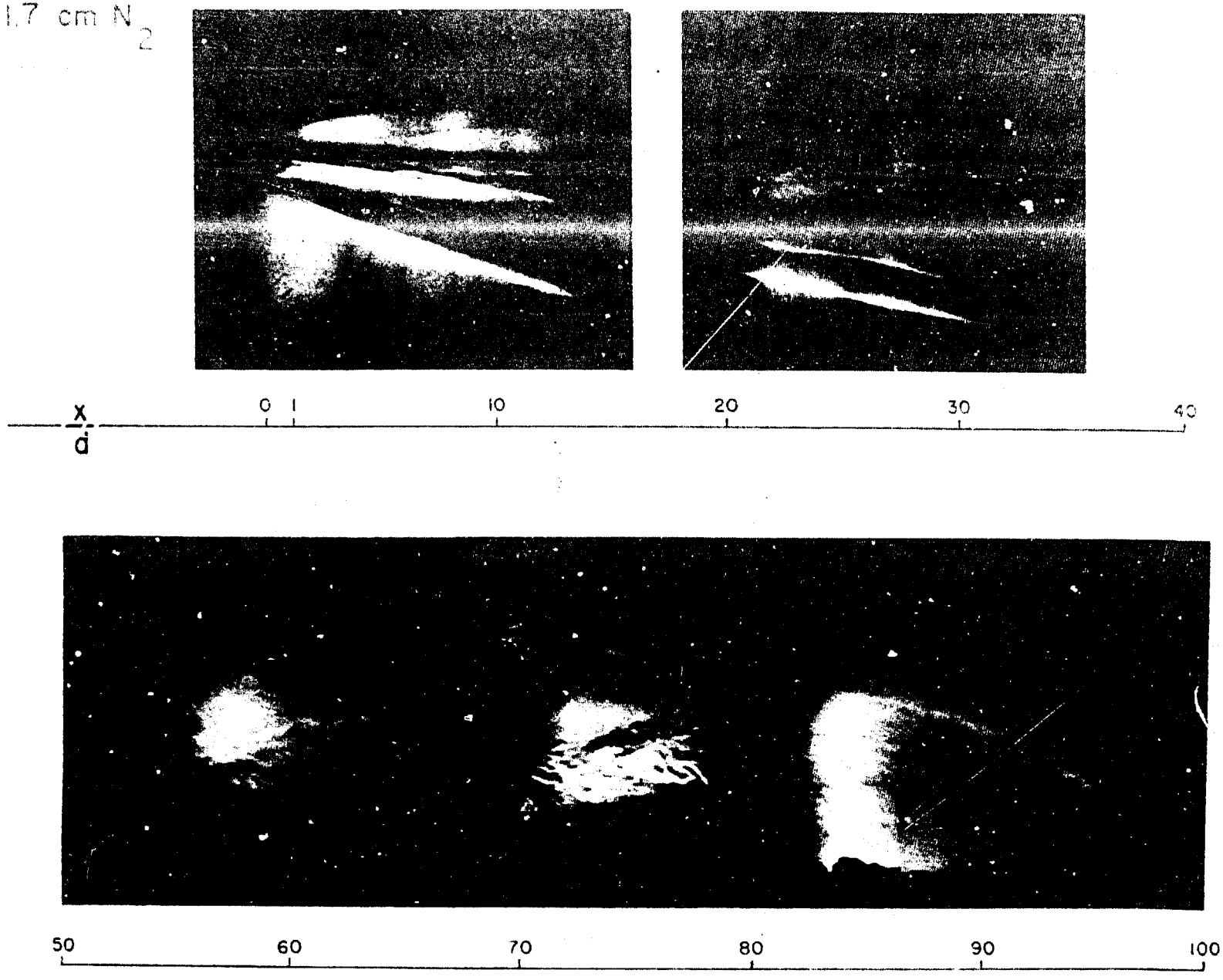

Fig. 1 Sodium schlieren composite of a 0.22-inch sphere hypersonic wake in nitrogen. Pressure = 1.7 cm Hg, V ≈ 14,000 ft/sec.

amplified to a large degree and the pattern looks more or less like vortex loops, one stacked behind the other, exhibiting the nearly periodic component to the flow. The next picture in the sequence shows some indication of the deterioration of the large scale vortex filaments as they fill up with small scale eddies. The last picture shows the continuation of this decay process towards fully developed turbulence. The shock waves seen in the last three pictures are reflections of the projectile's bow shock from the test section walls. This set of pictures near transition illustrates the origin, growth, and the beginning of the breakdown towards fully developed turbulence of hypersonic nonsteady wake flow.

Other sensitive schlieren systems omitting the sodium vapor modification have also produced photographs of hypersonic wakes and such data will be used in the following sections. At the Reynolds number corresponding to the data shown in Fig. 1, such schlieren photographs appear to show a rapid development of turbulence downstream of the body at a point 30 body diameters from the pellet.[9] Figure 1 suggests that what is seen at 30 body diameters downstream (second photograph) is the continued amplification of the small density gradient perturbations already present near the body in the zero to 10 body diameter region, as shown in the first photograph. It is suggested that the increased refractivity of the sodium resonance radiation has allowed us to detect weak density fluctuations where they first appear right near to the body. The threshold of the air schlieren systems used in other experiments may not have allowed observation of the original small fluctuations until after some fluid mechanical amplification. Only when the density gradients become sufficiently large to create a light fluctuation in such an air system will turbulent structure appear in such a photograph. Advanced schlieren techniques now confirm the gradual development of turbulence downstream.[41]

Figure 2 shows a photograph of the self-luminous wake (taken by the racetrack technique[10]) at a similar shoulder Reynolds number to the sodium schlieren results of Fig. 1. The luminosity of the near wake region appears to have a long wavy motion which downstream at about 30 body diameters

Fig. 2 Race track picture of a 1-inch diameter sphere hypersonic wake in air. Pressure = 7.6 mm Hg. V = 16,000 ft/sec. Taken at Canadian Armanent Research Defense Establishment. The length scale is a skewed cut across the x-t plane.[10]

develops into large scale, vortex filaments. This amplification of the near wake wave motion into large scale, vortex filaments shown by the racetrack technique in Fig. 2, is presumed to be the same process as the amplification of the small perturbations near to the body into vortex filaments evident by the sodium schlieren technique in Fig. 1. In this sense, both observations support the thesis that this amplification does not portray a sudden transition to turbulent flow. Rather, there is a hierarchy of flow patterns beginning in the body flow region and continuing downstream which lead to the fully developed turbulent wake structure.

Figure 3 shows a high quality shadowgraph behind a cone. The shadowgraph technique is sensitive to the second derivative of density and hence emphasizes smaller scale. Also, in the cone flow field, the entropy changes from the boundary layer-induced inner wake to the shock-induced outer wake are greater than in the sphere case. Thus, shadowgraphs of cone wakes in the transition regime may be expected to show more detail of the development of fluid mechanical unsteadiness than schlieren photographs of sphere wakes.[11] One sees in the details of wake transition in Fig. 3 the same sort hierarchy of unsteady flow regimes as described above in experiments with other diagnostics.

The hypersonic wake has three strong compressibility effects which must be considered in addition to the shape of the velocity profile: pressure gradient, Mach number, and lateral temperature variation. Tollmein[12] has shown that the existence of a point of inflection in the velocity profile is a necessary and sufficient condition for the amplification of infitisimal disturbances. In boundary layer flow with favorable pressure gradients, the velocity profile has negative curvature everywhere. Thus, these boundary layer flows have higher transition Reynolds numbers than those with adverse pressure gradients since the latter possess velocity profiles with inflection points.

Wake velocity profiles have inflection points a priori. Pretsch[13] has shown that the influence of the pressure gradient enters stability analysis only through the velocity profile, u(y). Thus, in considering the stability of wake flow with pressure gradient, one need only consider the pressure effect on the distribution of the velocity profile with y.

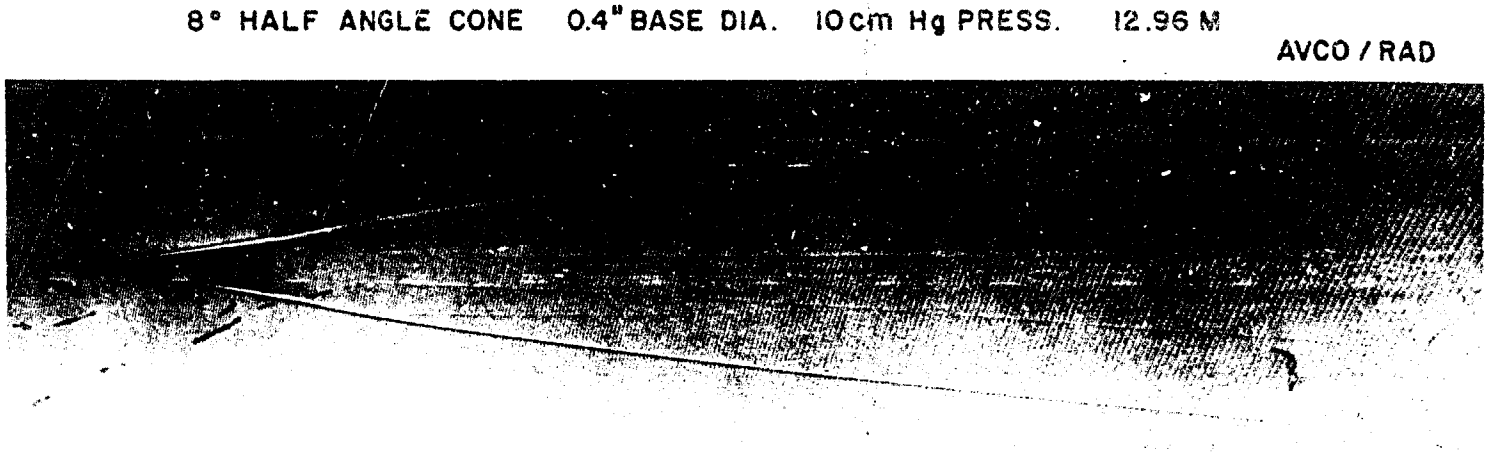

Fig. 3 Shadowgraph of Cone Wake. Naval Ordnance Laboratory. Courtesy of Avco/RAD.

In the near wake, the mean flow profiles change very rapidly and the inviscid stability characteristics (which are very sensitive to the mean profiles) of such flows will be different than those of the slowly varying far wake profiles. Gold[14] for two separate sets of "actual" (deviating somewhat from the Gaussian) near wake profiles found (1) that both allowed subsonic disturbances indicating possible neutral self-excited disturbances throughout the wake, and (2) that far downstream the "actual" wave speeds approached the "Gaussian" wave speeds.

The pressure gradient effect is naturally small as the pressure approaches the free stream value. In the blunt body case, blast wave theory gives an approximate downstream limit ($p = p_\infty$) for the pressure gradient effect as:[15]

$$\text{planar:} \quad p/p_\infty = 1 = 0.121 \frac{M_\infty{}^2 C_D{}^{2/3}}{(x/d)^{2/3}} + 0.56 \qquad (1)$$

$$\text{axisymmetric:} \quad p/p_\infty = 1 = 0.067 \frac{M_\infty{}^2 \sqrt{C_D}}{x/d} + 0.44 \qquad (2)$$

For slender cones, like total cone angle less than 30°, calculations show that the $p \rightarrow p_\infty$ point is close to the end of the recompression zone.

Solutions to compressible small amplitude eigen-value stability probelms cannot be found for supersonic disturbances of the fundamental mode. It is this fact which introduces the relative Mach number across the wake as a parameter in the hypersonic wake transition probelm. As a result, it is generally felt that only subsonic disturbances are important for instability;[16,17] i.e., for the wake, disturbances which are subsonic with respect to both the mean flow at the edge, u_e, and at the center line, u_ℓ. This is equivalent to saying that the disturbance signals must be able to reinforce each other and not die out at infinity. This concept expresses itself analytically[14] as

$$\bar{M}_{es} \equiv \frac{u_e - c_s}{a_e} < 1 \qquad (3)$$

for the development of instabilities, where c_s is the phase velocity of the disturbance in body coordinates. Numerical calculations by Gold indicate that for hypersonic flow this is satisfied not too far downstream of the body ($< 100\,d$) in both the blunt and slender body cases.

It should be pointed out that in recent work by Mack[18] on the two-dimensional problem, even when no neutral or self-excited subsonic disturbances corresponding to the fundamental mode exist, he found the existence of self-excited disturbances of the higher modes. Energy transfer for these modes may be provided by the "bouncing" of the waves back and forth within the supersonic region.

The effect of a hot wake core on the stability analysis is two-fold:[14] (1) As the wake core temperature excess increases, the range of relative Mach numbers over which unstable disturbances can exist also increases; (2) however, if the relative Mach number is less than M_{cr}, the amplification rates per wavelength for two-dimensional flows of a hot wake decrease significantly with increasing ΔT and are rather unaffected in the axisymmetric case.

For a blunt body, the condition in Eq. (3) is satisfied close to the recompression region well before the $p \rightarrow p_\infty$ position is reached. Thus, the end of the compressibility effects in hypersonic wake transition for blunt bodies is controlled by the pressure decay. For a slender cone one set of calculations show that at high altitudes, say from 100,000 to 200,000 ft, $\bar{M}_{es} > 1$ may persist for some several hundred body diameters downstream.[19] Thus, the end of the compressibility effects in hypersonic wake transition for cones is controlled by the $\bar{M}_{es}$ decay.

Since the compressibility effects are related to the hypersonic processes near to the body, the part of the wake which is dominated by these local details will be called the "Near Wake." By definition the "Far Wake" will be where the wake velocity profiles have reached their asymptotic behavior, property gradients have become small and details

of body shape have been lost. The Interpolation regime will be the regime where one traverses from the Near to the Far wake: where the strong favorable pressure gradient, the strong density gradients, and the effect of body shape all become less important as one proceeds downstream.

Before proceeding with analysis of the wake transition experiments, we discuss those cases where there has been injection of mass from the body into the wake. Such injection could be done deliberately, such as would occur in some types of boundary layer control methods, or could be the result of surface ablation. No laboratory experiments on this effect are available in the literature.

We can make certain remarks on what might be expected in the case of low mass injection rates into the flow field. We will assume, based on certain peripheral experimental information to be presented, that if the rate of mass injection is small relative to the rate of mass of air encountered by the body, that there is little ablation effect on wake transtion. This assumption has some theoretical base. Consider an experiment in wind tunnel coordinates. It is reasonable to assume that the injected mass leaves the body surface at small velocity relative to the fast free stream. Thus, the momentum balance for the control volume surrounding the body requires that all of the momentum gained by the injected mass in the free stream direction be lost by the free stream, which maintains the total drag of the body constant. (We neglect for this argument the effect of ablation on the boundary layer profile which will affect the skin friction drag.) Although the momentum defect passing out of the control volume (which is equal to the body drag) is unchanged, the velocity distribution may be locally altered so as to produce a more unstable profile. However, as Gold[11] has calculated, small differences in profile shape have small effects on growth of disturbances. Thus, the assumption of small effects when the ratio of injected mass rate to intercepted is small seems to be reasonable. Further remarks will be made at appropriate places in the following discussion for the effects to be expected in the case of high mass injection rates.

3. THE SPECTRAL OUTLINE FOR THE EXPERIMENTAL DATA

The spectral intensity of the wake fluctuations may be roughly divided between the discrete part at the characteristic frequencies (ordered) and the random part at all other frequencies (disordered). After the minimum critical Reynolds number has been passed, increasing the Reynolds number moves upstream the position at which some given distribution of wake fluctuations between ordered and disordered is found. Figure 4 illustrates this process schematically. For the present purpose of illustrative discussion, pressure decay, Mach number and temperature effects are neglected. The vertical axis represents the distribution of power between ordered and random (disordered) motion. The two axes in the horizontal plane are: (1) a representative Reynolds number, R_d; and (2) the distance downstream, x/d. The upstream progression is seen to be the locus in the horizontal plane corresponding to a given power spectral distribution (ordered-disordered). Lines obtained by planar cuts for the two other processes are also shown; the degradation of wake fluctuations down from the nearly ordered flow proceeding towards fully developed turbulence: (1) at fixed x/d with increasing R_d; and (2) at fixed R_d with increasing x/d. If pressure decay, Mach number, temperature and ablation effects are important, there is a separate surface in (R_d, x/d, spectral) space for each combination of values for these four effects.

It is useful to think of the experimental techniques employed for hypersonic wake transition work as mapping out different horizontal contours of the (R_d, x/d, ordered-disordered) surface. Close to the value (1.0 - 0.0) on the ordered-disordered spectral scale are techniques which are sensitive to property fluctuations or powers thereof. For example, self-luminous radiation is sensitive to a high power of temperature. Very slight fluctuations in temperature will produce perceptible structure in a self-luminous photograph. The appearance of structure in the self-luminous photographs with increasing R_d seems to have the characteristics of an "off-on" event.[8] Such would be the nature of the phenomenon represented by the horizontal locus corresponding to

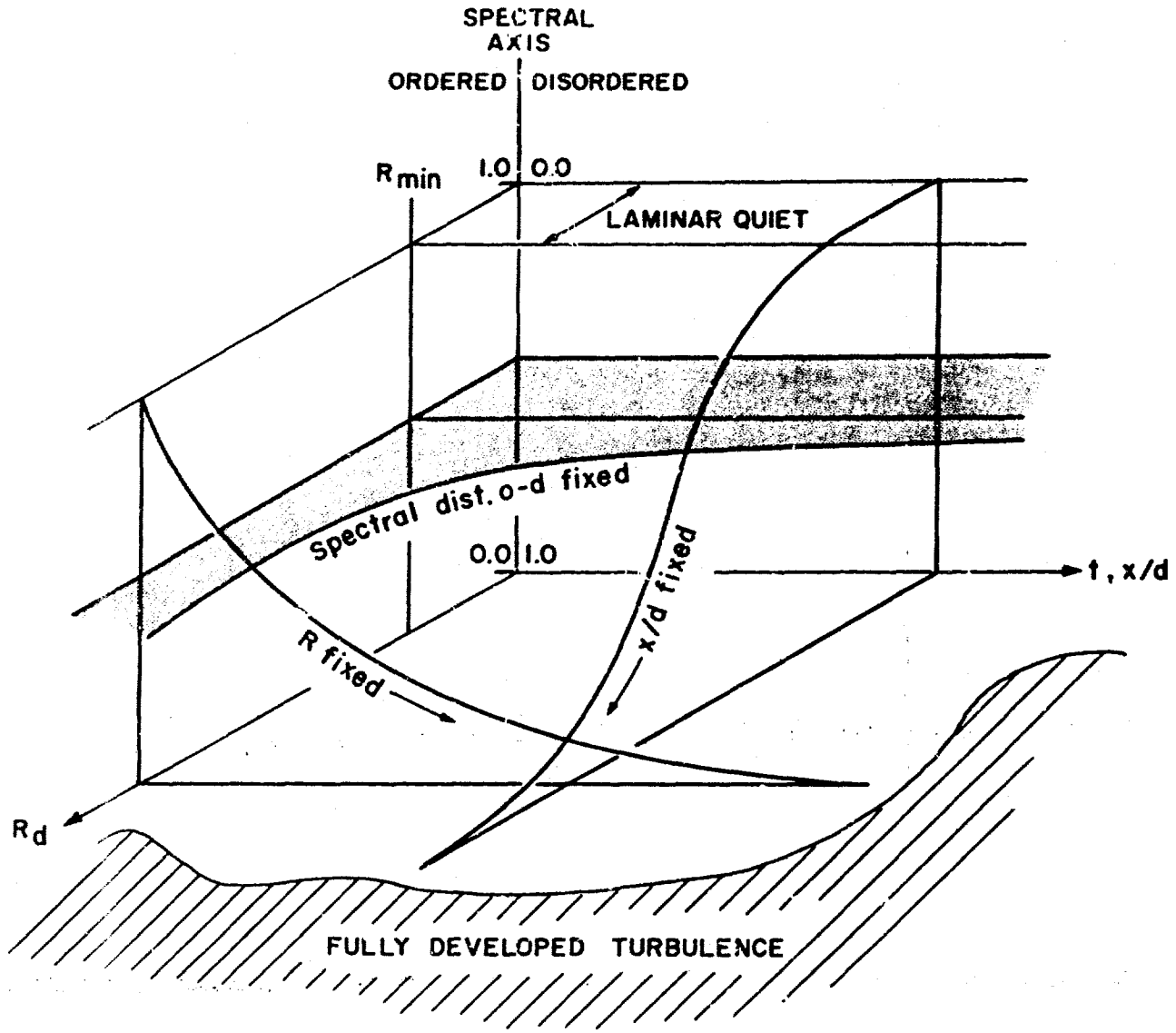

Fig. 4 Schematic illustration of development of turbulence.

a spectral value just below (1.0 - 0.0). Further down the spectral scale would be the interferometer technique which is directly related to density fluctuations.

Next down the spectral scale is the schlieren technique. The schlieren technique is sensitive to the first derivative of the density. Thus, the schlieren system registers unsteadiness when the density gradients (which are associated with the smaller scale eddies) become sufficiently sharp to create light fluctuations which are above the threshold level to produce structure in the schlieren photograph.

At still lower values on the spectral scale, comes the shadowgraph. The shadowgraph is sensitive to the second derivative of density and hence emphasizes still smaller scale eddies than the schlieren technique.

If these four optical techniques were used on the same experiment, each would map out the loci of points corresponding to four horizontal contours in Fig. 4. Unfortunately, it is not presently possible to obtain quantitative information about spectral distributions from all of these techniques. However, their relative locations with respect to each other on the spectral axis should be in the order in which they were discussed above.

Diagnostics in other parts of the electromagnetic spectrum are also used; e.g., microwaves, specially for hypersonic wake transition. Microwave data are for electron wake unsteadiness. It is most likely that fluid mechanical unsteadiness is a prerequisite for electron density unsteadiness. Thus, it is to be expected that fluid mechanical unsteadiness is as close or closer to the body than microwave data indicates. Further, the selected location of the beginning of fluid mechanical unsteadiness determined from visual examination of photographs is not sensitive to the wavelength of the unsteadiness at that point. However, the location of wake unsteadiness determined by microwave scattering is very sensitive to the scale of the electron density unsteadiness as represented by the refractive index fluctuations. The wake after having gone fluid mechanically unsteady may not produce the smaller electron fluctuation scale for microwave scattering until further down-

stream or until a higher ambient pressure is reached. Thus, at a given pressure, the relative location of microwave wake transition further downstream than the fluid mechanical observation is a reasonable state of affairs, even without considering the problem of electron production. The results of ballistic range experiments at General Motors Defense Research Laboratory[20] support this argument. Figure 5 shows this relationship for both sphere and cone experiments; that is, the microwave transition curve is further downstream or at higher ambient pressure than the curve traced out by the schlieren techniques.

Demetriades[21] used the integrated rms output of a hot-wire as a diagnostic in hypersonic cylinder wake experiments. For x_{tr}, he arbitrarily selected the location of either the enhancement or the maximum in the rms output. The $(R_d, x/d)$ locus traced by the criterion of the enhancement of the rms signal would correspond to a higher position on the spectral axis than the criterion of the maximum output. Hypersonic cylinder wake transition is different from that for three-dimensional bodies. In the cylinder case, time to pass information along the wake shear layer in the direction perpendicular to the two-dimensional planar flow is long compared with time to pass information across the layer and with time to flow downstream around the body. This is not the case for wake shear layers of bodies of revolution. Thus, the details of cylinder hypersonic wake transition are different from those in the axisymmetric case and the cylinder case is not treated here. The concepts used in this paper to analyze hypersonic wake transition for bodies of revolution were actually developed first for cylinder wake transition. The results are qualitatively, though not quantitatively, the same.*

To locate the $(R_d, x/d)$ locus at its actual spectral value, one would have to resolve the fluctuation spectrum. Roshko did this with hot wire techniques in low speed cylinder wake experiments.[22] So far this has not been done in hypersonic experiments, although a start has

* Goldburg, A., Unpublished prepared comment presented on Demetriades' 1963 paper[21], AIAA Hypersonics Conference, Cambridge, Mass., August 1963.

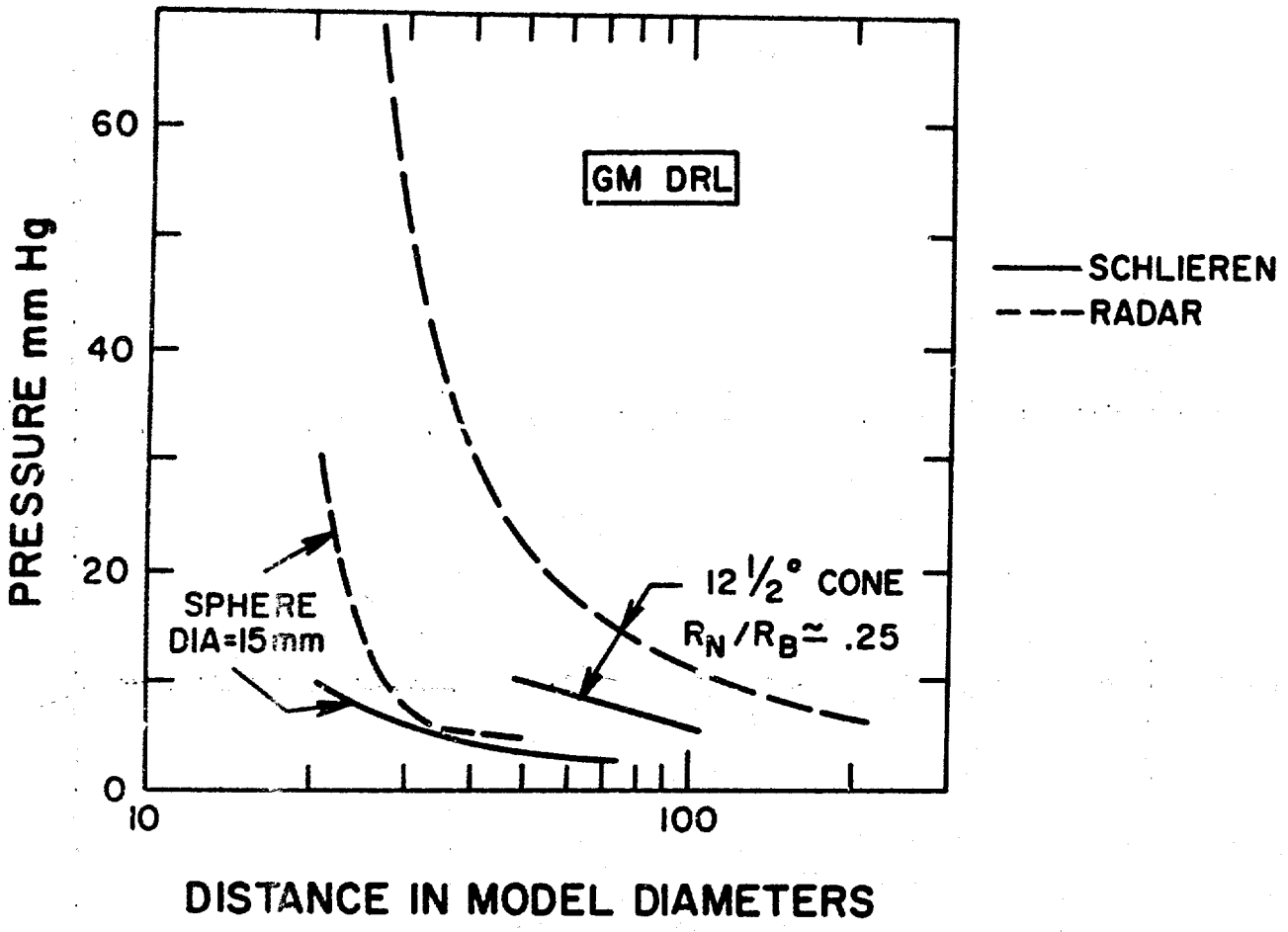

Fig. 5 Comparison of schlieren and radar wake transition location for both spheres and cones. (General Motors Defense Research Laboratory, Ref. 20, Fig. 10)

been made by Kendall at JPL[23] and Hromas at TRW.* However, it is possible to qualitatively relate the results of Roshko to the data obtained from schlieren diagnostics in ballistic ranges.

Slattery and Clay[9] carefully analyzed their schlieren photographs of hypersonic wakes in the transition regime. For each ballastic range shot they measured the distance, x_s, from the body to the point where, to their schlieren-eye-mind analysis system, some perceptible amount of structure could be seen in the photograph; e.g., see Fig. 3. Figure 6 includes a presentation of their data for spheres at $M_\infty \approx 7.5$. The ordinate is x_s/d and the abscissa is $R_d)_{shoulder}$, the Reynolds number calculated for conditions corresponding to those on the centerline streamline after it goes through the shock, around the nose and is turned back to horizontal. For blunt bodies, this is 90^o from the stagnation point vertical and for cones this is one-half the total cone angle from the end of the cone surface. The shoulder flow conditions are taken as typical of the near wake flow conditions. The local Reynolds number per unit length along the edge of the viscous core in the near wake is more or less constant and is near the shoulder value for blunt bodies and equal to that for slender cones. Since the shoulder values are easier to calculate and correspond to a definite position in space, the shoulder conditions are chosen for convenience and for certain reasons which will become apparent later on.

x_s is considered in this paper in the sense of being that downstream distance required for the development of unsteadiness into that degree of turbulence with sufficient sharpness of density gradient fluctuations to register above the threshold level of the diagnostic technique. It is assumed that this degree of turbulence corresponds for each separate reading (each separate run) to some unknown but more or less constant value on the spectral axis, Fig. 4. Thus, the data in Fig. 6 is looked upon as mapping out some particular horizontal contour of the $(R_d, x_s/d,$ spectral) surface: $f(R_d, x_s/d) = 0$.

From the quantitative hot-wire fluctuation spectral data given by Roshko,[22] it is possible to draw the curves for his low speed experiment for the 80 percent - 20 percent (ordered-disordered) plane and the 20 percent-80 percent (ordered-disordered) plane. It is seen in Fig. 6

* Private communication, L. Hromas, September, 1966.

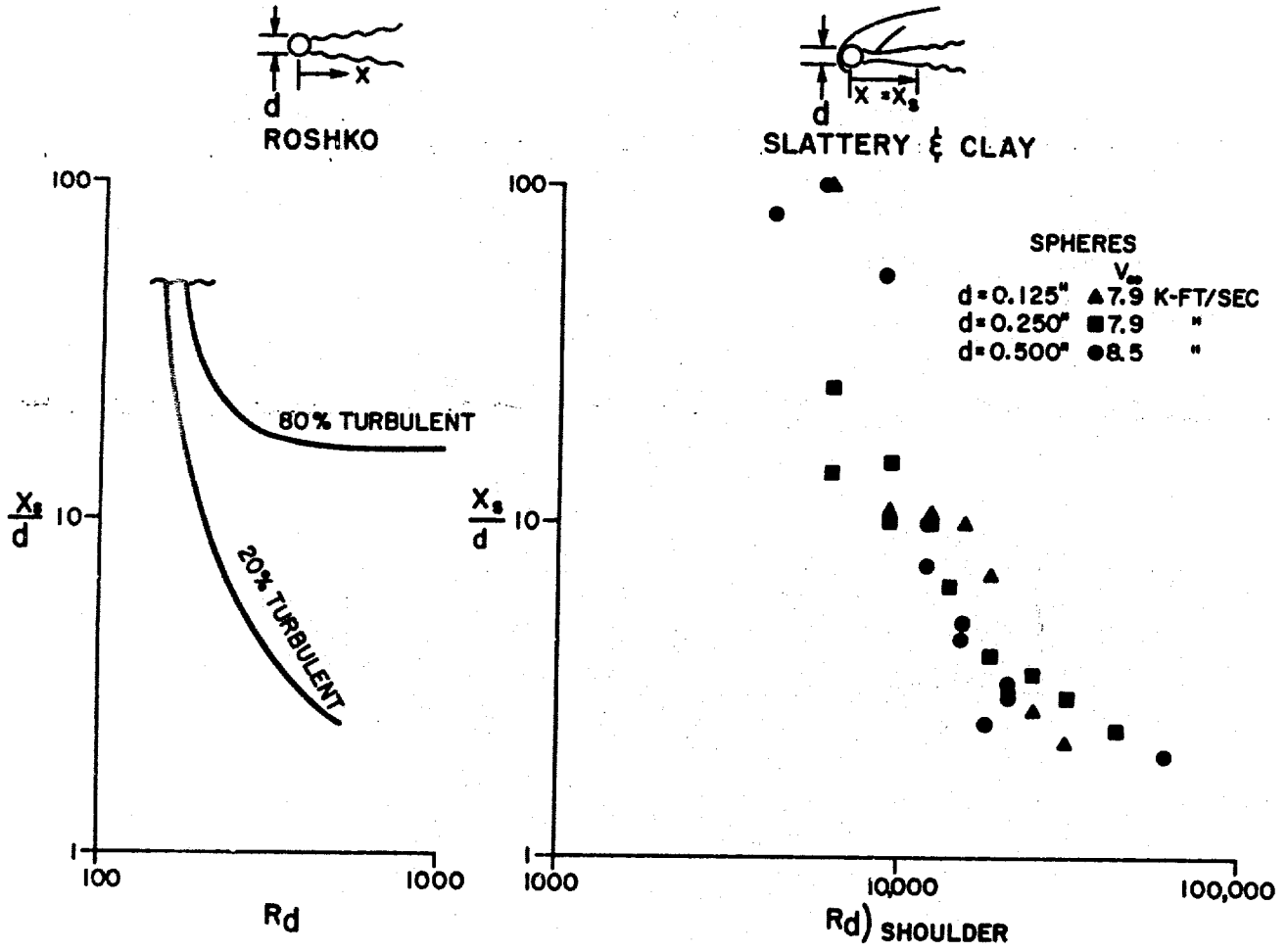

Fig. 6 Comparison of x_s/d, R_d data for hypersonic[9] and low-speed experiments.[22] Curves for Roshko's incompressible cylinder results are from his hot-wire spectral data.[8]

that the shape of the hypersonic transition curve $(x_s/d, R_d)$ is exactly similar to the loci of points traced out by the results of the quantitative hot-wire data in the low speed experiments of Roshko. Thus, we are encouraged that the spectral framework for the data as illustrated schematically in Fig. 4 is appropriate for an analysis of the hypersonic wake transition experiments.

4. THE CONCEPTUAL OUTLINE FOR THE SCALING LAWS

Hypersonic wake transition derives its separateness from low speed wake transition from the fact that in hypersonic wake transition there are two wakes left by the body: the shock-induced wake and the boundary layer-induced wake, Fig. 7. The author prefers this nomenclature due to its specific nature, clearly labelling the origin of each vortical flow and the mechanism for drag deposition in the flow field. Other names in use respectively are: outer-inner, entropy-viscous; and inviscid-viscous. The author feels that the last two are clearly misnomers and are definitely misleading to a large number of interested technologists, in that both wakes are "entropy" and "viscous" wakes, and that the shock-induced wake is clearly not without viscosity. The "entropy" wake is so-called because for blunt bodies most of the shock drag is produced by the part of the shock within the sonic line which is where the large entropy change takes place across the shock. However, in the case of slender bodies most of the entropy change takes place in the boundary layer and so this nomenclature is not appropriate. The "inviscid" wake is so-called because in calculating normal forces on bodies in supersonic flow, it is customary to separate the flow field into a "free stream", in which viscous effects are dropped as unnecessary for the normal surface force problem, and into a boundary layer where viscous effects are used to satisfy the tangential no-slip condition at the surface. However, the wake transition problem is a free shear layer problem in a real gas possessing finite viscosity involving a transition Reynolds number, and should not in any sense be spoken of or thought of as being "inviscid", without viscosity.

There is a part of small disturbance theory associated with the Orr-Sommerfeld equation in which the viscous terms are dropped.[24] The

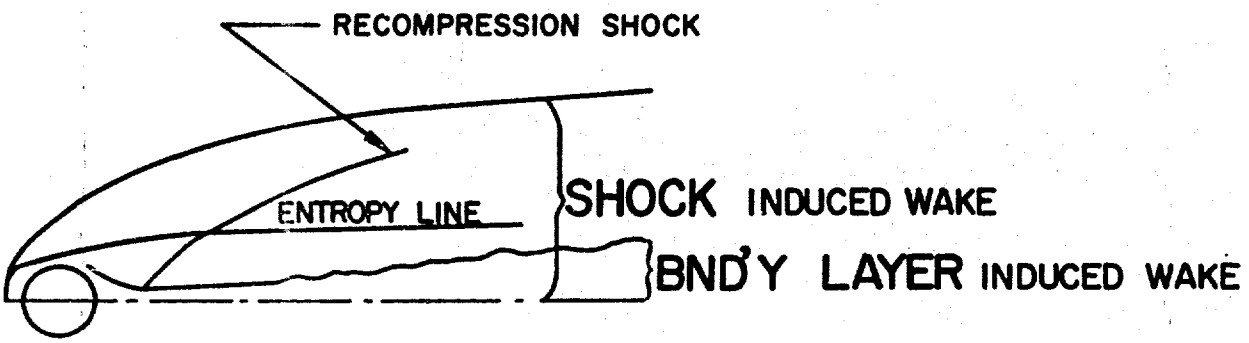

Fig. 7 Flow field nomenclature. Shock-induced wake (SiW) and boundary layer-induced wake (BLiW).

mathematical problem of an "inviscid" stability calculation must be recognized as associated with laminar flow which are solutions of the full Navier-Stokes equations where the influence of viscosity on the mean flow has been taken into account. What is neglected in the inviscid infinitesimal small disturbance theory is the influence of friction on the infinitesimal fluctuation. Of course, as soon as the fluctuation builds up into finite size in the non-linear amplification regime going towards turbulent transition, viscosity plays a role. Therefore, in discussing transition, the use of the "inviscid" nomenclature is unfortunate and will not be used here.

With two contiguous wakes, the shock induced wake (SiW) and the boundary layer induced wake (BLiW), there are three transition possibilities: 1) the SiW has gone unsteady and the BLiW has not; 2) the BLiW has gone unsteady and the SiW has not; 3) both wakes have gone unsteady either in unison or in separate motion. It is possible that when one wake has gone unsteady it may "trip" the other. For example, Fig. 8, a self-luminous racetrack photograph, shows both wakes evidently in unsteady sinuous motion, each independent of the other. By using xenon as the test gas, very high free stream Mach numbers ($M_\infty \approx 25$) were obtained, and hence very high flow field temperatures were produced behind the bow shock. This produces gas luminosity in the SiW as well as the stronger luminosity produced by the vaporized ablation products in the BLiW, thus visually distinguishing between the two wakes. Evidence in support of the possibility of the SiW being in unsteady motion independently of the BLiW was first given by Fay and Goldburg (Ref. 8, Section E).

With the above nomenclature and with the delineation of the wake by definition into three parts: Near Wake, Interpolation, and Far Wake, we next build a conceptual outline for the experimental data.

The Reynolds number will be adopted as the correlating non-dimensional parameter for the wake transition studies: This is taken directly from all previous fluid mechanical studies and experience. It is the primary parameter derived from the non-dimensionalization of the Navier-Stokes equations of motion,[24] and has had great usefulness in the

PRESSURE:0.8cm XENON
VELOCITY:13,200 f.p.s.
LEXAN PELLET

Fig. 8 Luminous undulating hypersonic wake with the SiW and the BLiW in apparently uncorrelated time-dependent motions.

study of transition in boundary layers, jets and incompressible wakes.[25] The numerical value of the Reynolds number is determined by the local properties characteristic of the flow in the vicinity of transition.

In the Far Wake, the fluid has relaxed its memory of the details of the way in which momentum was lost to the body (wind tunnel body fixed coordinates will be used unless otherwise stated). The velocity, density and temperature gradients have become small; the property distributions have reached their asymptotic shape. For laminar flow, the BLiW by molecular diffusion has spread out and smeared itself into the SiW so that the profiles show no sharp gradients within the interior of the total wake.

In the Far Wake, it will be postulated that the whole wake goes unsteady together at some unknown station or series of stations way, way downstream. This will be the first onset of wake unsteadiness, $x_{tr} \sim \infty$, and the total shear layer representing the whole momentum defect equal to the total drag of the body will participate in the transition. Thus, the appropriate length scale will be the total $\sqrt{C_D A}$ of the body, or equivalently the total momentum thickness of the total wake, θ, being a sum of that of the SiW and the BLiW. Thus, the Reynolds number for transition to unsteadiness in the Far Wake will be based on $\sqrt{C_D A}$: $R_{\sqrt{C_D A}} = \text{constant}$. Figure 9a presents this discussion schematically. The shaded area represents the diffusion of the BLiW into the SiW, thus effectively making one wake with total momentum defect equal to the total drag of the body.

In the Near Wake, the two wakes are clearly delineated by sharp property gradients across the edge of the BLiW. The two wakes have strong memory of their past origins and are strongly influenced by the local details of the flow field around the body. It has been observed that to schlieren diagnostics the SiW usually appears smooth in this region, while the BLiW has gone unsteady. In the schematic this state of affairs is represented in Fig. 9b. It can be seen in such a case that it may be possible for the BLiW to be unsteady and for the SiW at very high entropies to be opaque to the diagnostic. In such a case as this, the diagnostic would not be able to follow the upstream

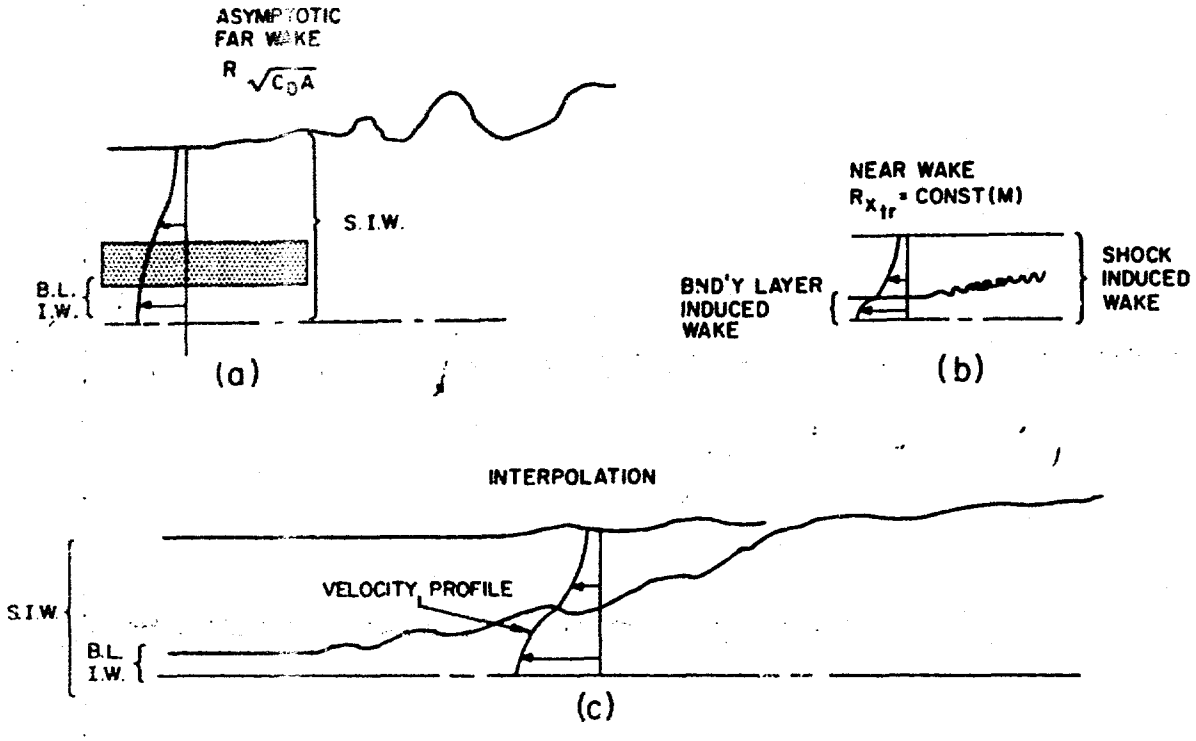

Fig. 9 Schematic of Far, Near and Interpolation Wakes.

movement of the x_{tr} beyond the point where the unsteadiness enters within the high entropy region of the SiW, which remains steady. In other words, if the steady entropy region of the SiW is opaque to the diagnostic, the unsteady BLiW would not be apparent until it broke through the "entropy" line. Laboratory evidence for this phenomenon was first obtained by Wilson.[26]

In the Near Wake, local hypersonic phenomena depending on body shape dominate the flow field as is the case for all body related shear layers — boundary layers and separation shear layers. Hidalgo,[27] and Professor Lees and his graduate students[21] extended the transition correlation ideas developed for body related shear layers and proposed that the wake transition correlation length would be the distance from the origin of the Near Wake to the transition point. For convenience, the origin for x_{tr} is taken from the base of the body. The end of the recompression region might be more appropriate, but since values of x_{tr} of interest are usually greater than two body diameters downstream, and since the correlations to be developed will be valid to no better than a factor of two, the choice of origin is not critical since the recompression region itself is like one or two body diameters downstream.[28] Further, by continuing analogy they suggested that R based on x_{tr} would be a strong function of the local Mach number at the edge of the BLiW at the location of x_{tr}, M_e. Thus, $R_{x_{tr}}$ equals a constant, C_M, which varies with M_e.

In the Interpolation regime, one traverses from the Near to the Far Wake. Going downstream, the strong favorable pressure gradient, the strong density gradients, the large Mach number and temperature changes across the boundary layer and shock-induced wakes decrease and become less important. Going upstream in this region, the wakes begin to take on their separate characters and the unsteadiness becomes more and more to be located mostly in the BLiW. This situation is represented schematically in Fig. 9c.

In the Interpolation regime, the Navier-Stokes equations will be used with certain simple arguments to derive an interpolation curve to go from the $R_{\sqrt{C_D A}}$ correlation of the Far Wake to the $R_{x_{tr}}$ correlation of the Near Wake. The simplest such interpolation formula is

$$\left(C_M / R_{x_{tr}}\right)^a = \left[1 - \left|\left(R\sqrt{C_D A}\right) \Big/ R\sqrt{C_D A}\right|\right] \qquad (4)$$

$(\ )_T$ is the transition value for the onset of Far Wake transition and a is some fitting parameter to be determined by the data. Thus, consider a given body in a given flow field: For onset of wake unsteadiness far downstream in the Far Wake (Fig. 9a) $x_{tr} \to \infty$, the Far Wake law is obtained

$$R\sqrt{C_D A} = \left(R\sqrt{C_D A}\right)_T = \text{constant} \qquad (5)$$

For R per unit length increasing to very large values, x_{tr} decreasing, the transition point moving towards the body, the Near Wake law is obtained.

$$R_{x_{tr}} = C_M \qquad (6)$$

At a given flight velocity for gas mixtures governed by binary collisions, it is possible to represent the Reynolds number as the free stream pressure times the characteristic length. Thus, the hypersonic wake transition laws become

$$\text{Far Wake:} \quad p_\infty \sqrt{C_D A} = \text{constant} \qquad (7)$$

$$\text{Near Wake:} \quad p_\infty \cdot x_{tr} = \text{constant (function of } M_{sh}) \qquad (8)$$

M_e, the local Mach number at the edge of the BLiW is here replaced by the Mach number at the shoulder of the body after the flow has been turned back to the horizontal, M_{sh}, see sketch in Fig. 10. Since in the near wake region, M_e does not vary significantly as a function of distance downstream along the BLiW edge, and since the local Mach number at the shoulder of the body is close to M_e, M_{sh} is selected here as being sufficiently characteristic of the local hypersonic flow field in the region near the particular shaped body.

The correlations (7) and (8) lend themselves to presentation on a log-log plot with x_{tr} as ordinate and p_∞ as abscissae, Fig. 10. Thus,

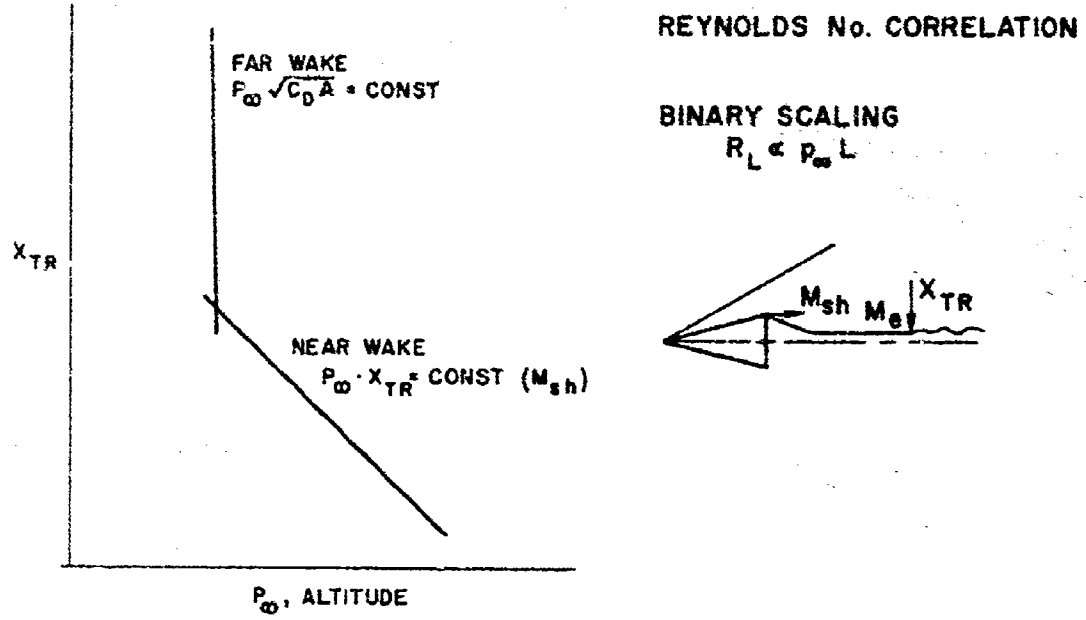

Fig. 10 Outline of the Hypersonic Wake Transition Map based on binary scaling.

A4296

for the Far Wake law (7), the p_∞ determined for the total $\sqrt{C_D A}$ body is a pressure below which the wake will always remain steady. Or, for the Far Wake law (7), to each value of p_∞ (altitude), there is assigned a value of $\sqrt{C_D A}$ such that any body possessing that total drag area will produce unsteadiness somewhere in its Far Wake at that altitude.

Next, the Near Wake law (8) on such a plot becomes a series of straight lines with negative one slopes, a separate line being assigned for each value of $M_{shoulder}$.

The task is now clear. The constants in Eqs. (7) and (8) must be determined so that the hypersonic wake transition correlation map may be constructed in a quantitative manner. These constants are determined from the laboratory ballistic range data in the next two sections, 5 and 6. In addition, the necessary interpolation curves must be structured from the ballistic range data. This is done in Section 7.

5. THE FAR WAKE CORRELATION

The Far Wake is that region where all details of the body shape have diffused away. Only the SiW is discernible, the BLiW having diffused into it, Fig. 9; all that remains is information about the total momentum defect deposited by the body ~ $C_D A$. Transition in the Far Wake is here characterized as an off-on phenomenon. As indicated in Fig. 10 we wish to find for each free stream pressure, p_∞, a size of body whose wake will show unsteadiness somewhere very far downstream as that pressure threshold is passed. In this step, no attention is paid to the hierarchy of the transition modes. A scaling law is sought for the onset of wake time dependency in terms only of the total momentum defect deposited by the body drag.

Results from incompressible flow[29] indicate that the total $\sqrt{C_D A}$ left by the body is the correlating length parameter independent of the means of deposition; i.e., regardless of the details of the combination of normal pressure, skin friction, base and induced pressure drags. Arkhipov[30] performed the small disturbance stability analysis for a planar wake with velocity profiles taken from the Tollmein's solutions.[12, 24]

The results of his wake stability analysis show that the parameter which characterizes a transition of the flow to a state of instability is Reynolds number based on total wake momentum thickness: $R_\theta \approx 24$, where momentum thickness is related to $C_D A$ by

$$\rho_\infty U_\infty^2 \pi^j \theta^{j+1} = \text{Drag} = 1/2 \rho_\infty U_\infty^2 C_D A \quad \begin{cases} j = 0 = \text{planar} \\ j = 1 = \text{circular} \end{cases}$$

The suggestion that the onset of wake unsteadiness is characterized by a transition value of R_θ, independent of the mechanism of drag production, is also supported by experimental work on cylinders and flat plates. For cylinders, wake transition occurs at $R_d \approx 50$, with corresponding $R_\theta \approx 42$ (Ref. 25). At this value of Re_d, the total drag is divided approximately half and half between pressure (form) drag and skin friction drag (Ref. 25, Fig. 154). For flat plates of length ℓ, Taneda's experiments[31] give wake transition at $R_\ell \approx 1000$, with corresponding $R_\theta \approx 44$. In the case of the flat plate the total drag is produced by skin friction alone. The fact that Arkhipov's theoretical value is lower than the experimental values is to be expected since the experiments deal with transition to finite unsteadiness whereas the theory deals with the onset of amplification of infinitesimal disturbances. Another consideration is that the theoretical work assumes for the velocity profile an asymptotic Gaussian form; whereas in the experiment, the instabilities may develop nearer to the flat plate where the velocity profile is not Gaussian. The actual velocity profile at the onset of amplification may give a higher theoretical R_θ transition than the result developed from the assumed Gaussian shape.

In Goldburg and Florsheim,[29] transition in incompressible wakes of three-dimensional bodies was considered: spheres and slender cones of various cone angles. They showed for the three-dimensional case that although the $(R_d)_T$ for the bodies tested varied by a factor of two, when the total momentum thickness or $\sqrt{C_D A}$ was used as the length parameter for onset of wake unsteadiness: $(R_\theta)_T = 95$ was a correlation to better than 10 percent.

Thus, there is theoretical and experimental support for correlating the onset of hypersonic Far Wake unsteadiness with the Reynolds number based on a length parameter characteristic of the total drag area of the body represented by the total momentum defect across the whole SiW, including the diffused BLiW. (This correlation was first used for hypersonic wakes by W. Schultis in an unpublished report: Study of transition from laminar to turbulent flow in wakes, Nov. 1961.) The ballistic range laboratory data for all ballistic range experiments available in the open literature is plotted in Fig. 11 to determine empirically the constant in Eq. (7), $p_\infty \sqrt{C_D A}$ = constant.

Consider first the drum camera photographs of self-luminous wakes.[8] These data characteristically show either a smooth diffuse texture or show gradients in the luminosity (Fig. 12). As a function of increasing free stream pressure, luminous structure is either absent or then present. No upstream motion of structure with increasing Reynolds number is usually seen. The absence or presence of luminous structure with increasing Reynolds number seems to have the character of an off-on event, as if the transition "snapped-in" from very far downstream almost instantaneously. Such would be the character of the phenomenon represented by the horizontal locus corresponding to a spectral value just below (1.0 - 0.0) on the ordered-disordered spectral scale in Fig. 4.

It is suggested that self-luminous radiation structure in the near wake is a sensitive test for onset of finite transition in the Far Wake. The reason for this suggestion is that radiation goes as a very high power of the temperature. Any small anomalies in temperature will give rise to greatly amplified structure in the radiation pattern. Thus, very small flow field anomalies in the Near Wake, which will be amplified into the onset of finite unsteadiness in the Far Wake, may be detectable in the Near Wake with self-luminous radiation. Figure 10 sets forth the transition information in air for the self-luminous diagnostic on a $p_\infty \sqrt{C_D A}$ and U_∞ plot. Laminar corresponds to a self-luminous photograph without structure; turbulent, with structure; and intermediate means that the observer could not make a definite determination because of some very slight indications of unsteadiness.

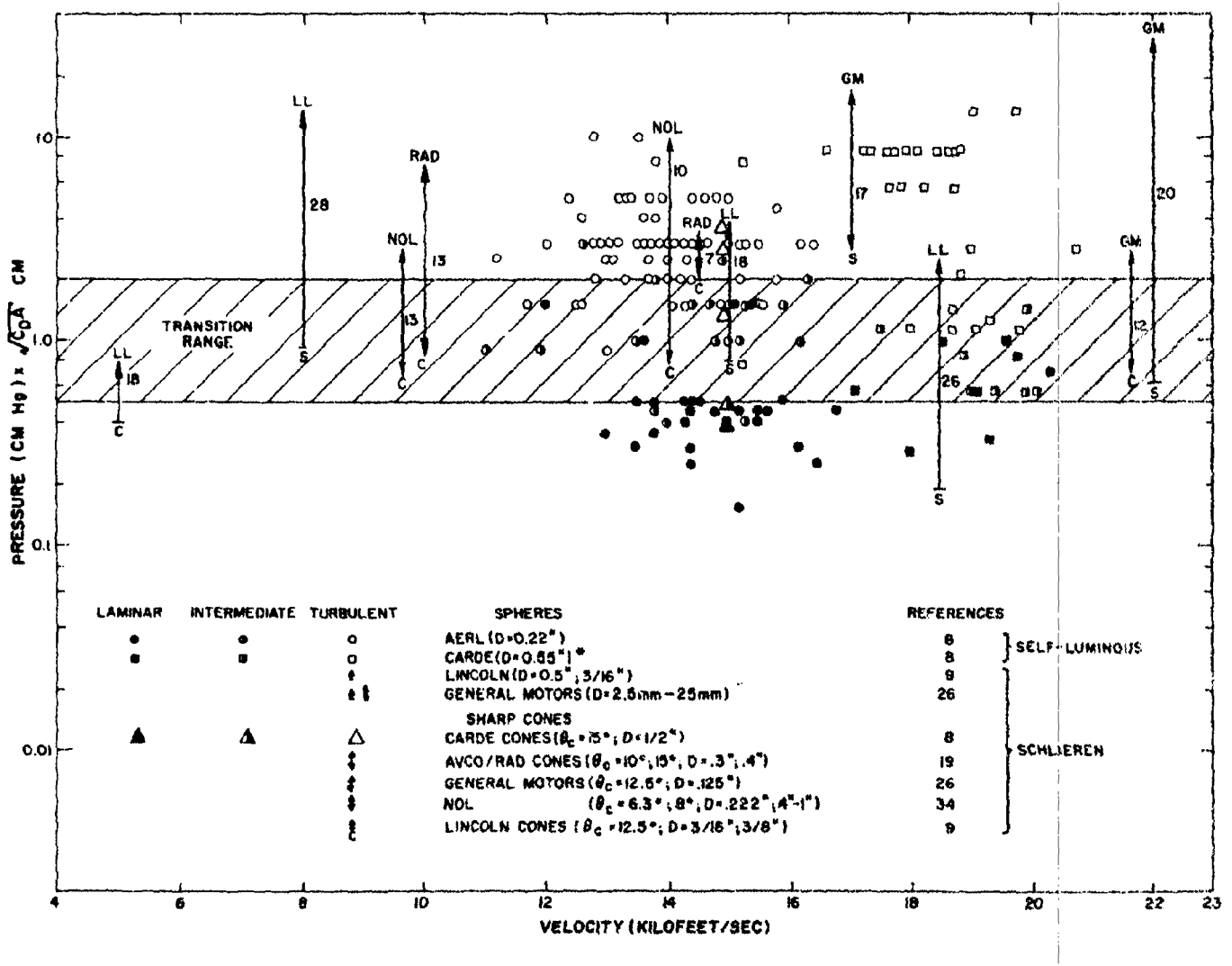

Fig. 11 Far Wake Transition Correlation. All available experimental information for air in open literature. CARDE vehicle was a sphere-cylinder-sphere: $\ell_{cyl} \approx r_{sphere}$.

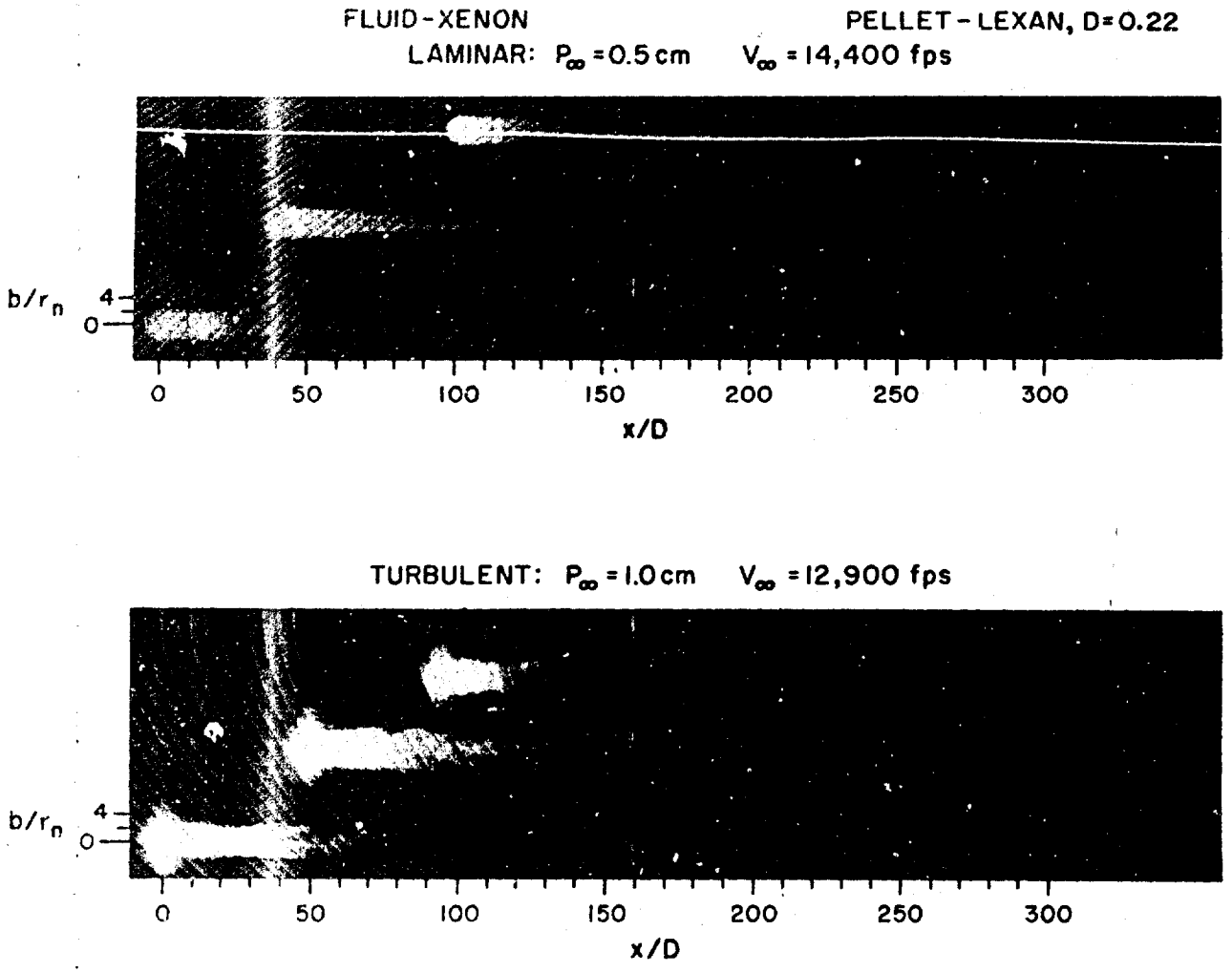

Fig. 12 Racetrack photographs of luminous hypersonic wakes. d = 0.22".

The schlieren values for transition were obtained by the investigator laying a marker on the photograph where perceptible unsteady structure in the wake was apparent, Fig. 3. These data all showed the behavior as represented in Fig. 6. Thus, as ambient pressure was decreased from run to run, the x_{tr} or x_s marked by the investigator moved further and further back in the wake until some minimum pressure was passed below which no structure was ever apparent in the wake. The schlieren data are represented in Fig. 11 as a vertical line at the approximate velocity of the set of experiments. At the top of the line are the initials of the performing laboratory. At the bottom is S or C, for sphere or cone data. Beside the line is the number of runs represented. The top of the line is terminated with an arrow at the highest value of $p_\infty \sqrt{C_D A}$ for that set of experiments. The arrow indicates that the wake would continue turbulent with increasing values of $p_\infty \sqrt{C_D A}$. Obviously, this limit could be pushed higher and higher, eventually producing transition in the body boundary layer. If a lower asymptote is reached for a minimum pressure (Reynolds No.) for transition, such as shown in Fig. 6, the arrow is terminated at the minimum $p_\infty \sqrt{C_D A}$ of the experiment set with a horizontal mark. For example, the line at 8000 ft/sec represents the data in Fig. 6. If no minimum asymptote appears on such a plot as Fig. 6, the line is terminated at the bottom with a downward facing arrow indicating that the experiment set did not proceed to low enough values of $p_\infty \sqrt{C_D A}$ to reach the disappearance of wake unsteadiness.

Figure 11 includes all available laboratory ballistic range data. Transition is a statistical phenomenon and the off-on characterization used for the Far Wake lends itself to a probability analysis. The transition results of Fig. 11 give

MEAN	$p_\infty \sqrt{C_D A}$	= 1.0 cm x cm Hg
1σ		= $\pm$ 0.5
2σ		= $\pm$ 0.75

We choose here to take the low 1σ value as the constant for the Far Wake transition correlation of Eq. (7).

$$p_\infty \sqrt{C_D A} = 0.5 \text{ cm Hg x cm}$$

(9)

$$\left(p_\infty / p_{sl}\right) \sqrt{C_D A} = 2.2 \times 10^{-4} \text{ ft}$$

It is emphasized that the $\sqrt{C_D A}$ in the Far Wake correlation (9) is the total $\sqrt{C_D A}$ and corresponds to all of the drag in the SiW and in the BLiW, the latter having diffused in some fluid mechanical sense into the former in the Far Wake such that they both go unsteady as a whole or, if still discernible, together. This correlation is meant to include angle of attack effects as well, so long as total $\sqrt{C_D A}$ at the angle of attack is used in the correlation.

The use of ablating bodies (the self-luminous photographs depend on the luminosity of the ablation products for the observable diagnostic) for transition work is questionable. However, in these experiments with small ablation rates (calculations show that for these experiments the ratio of the mass rate of ablation with respect to the mass rate of air encountered is less than $0(10^{-2})$.) the transition value of $p_\infty \sqrt{C_D A}$ does not vary between individual sets of experiments with and without ablating bodies. If ablation rates were large, like of the order of the mass rate of air encountered, one might expect (1) either an alteration to the characteristic length used (perhaps including some characterization of the "force", $\dot{m}_{abl} U_\infty$, divided by $1/2\, p_\infty U_\infty^2$ to make an additional "length"[32]) or (2) an alteration which is a function of the ablation rate to the value of the constant in the Far Wake law. Qualitative experiments by Wilson[26] support the above arguments.

Since free shear layers are extremely unstable and have critical Reynolds numbers of the order of 10, rarefaction effects may be important. Representing the Reynolds number by Mach number times the inverse of the Knudsen number, we see that for high Mach number flows,

say like the order of 10, that the Knudsen number is like order one. Thus, hypersonic wake unsteadiness occurs very close to the end of the continuum flow regime, if not somewhat into the rarefied flow regime. The scaling constant given in Eq. (9), based on ballistic range data, assumed for spheres and cones the continuum value of C_D. It may be that $C_D > C_{D\,\text{continuum}}$ at the onset of wake unsteadiness by 10 or 20 percent.

In conclusion, it is pointed out that the correlation constant of Eq. (9) is good only to like a factor of two. This is readily seen in Fig. 11 where the transition region is shown shaded to a factor of two either side of the mean. For hypersonic transition work this is quite usual. For example, the transition Reynolds number for heat transfer to blunt nosed bodies in hypersonic flow is also known only to a factor of two.[33] What one is dealing with in compressible turbulent transition is a random, spectrally disorganized highly nonlinear process, the onset of which is decidedly influenced by the anomalies in the steady-state condition of the ambient environment.

6. THE NEAR WAKE CORRELATION

In the Near Wake, local hypersonic phenomena depending on body shape dominate the flow field. The strong favorable pressure gradient, the large temperature and Mach number differential across the SiW tend to stabilize it. Usually only the BLiW is observed to go into finite unsteadiness in schlieren and shadowgraph photographs. The SiW is like a smooth sheath around the corrugated BLiW and for the electromagnetic scattering observable could specularly reflect the signal and thus shield the BLiW from the radar diagnostic.

As explained in Section 3, the point at which the investigator lays down the marker on the schlieren photograph to mark the onset of finite unsteadiness in the BLiW is considered here in the sense of being that downstream distance required for the development of disorder in the flow with that degree of turbulence which possesses sufficient sharpness of density gradient fluctuations to register above the threshold level of the diagnostic technique. It is assumed that this degree of turbulence corresponds for each separate reading (each separate run

of each separate investigator) to some unknown but more or less constant value on the spectral axis, Fig. 4. Thus, we assume that the Near Wake schlieren data are information on how some level of non-discrete fluctuating power moves upstream with increasing Reynolds number.

It is common for transition in Mach number stabilized body-related free shear layers that the hierarchy of fluid mechanical states from laminar to fully developed turbulence is compressed into a very small streamwise distance, of the order of two or three shear layer thicknesses. This corresponds to the sharp drop off in percentage ordered motion with x/d at high R_d in Fig. 4. This is in contradistinction to Far Wake transition, where the streamwise distance for transition may be of the order of several hundred shear layer thicknesses. This corresponds to the gentle drop-off in ordered motion with x/d at low R_d in Fig. 4. The fact that most flow visualization data of the wake transition process is in the near wake has misled many people into believing that transition is an apriori precipitous process. The whole concept of x_{tr} for wakes is largely due to an overemphasis on near wake transition pictures.

Hidalgo at Avco Everett[27] first suggested and Demetriades and Gold[21] first demonstrated conclusively that the $R_{x_{tr}}$ = constant correlation employed in transition of body related shear layers could be carried over to the near wake. The strong dependence of this correlation on local wake Mach number, M_e, at the point of wake transition (also suggested by Hidalgo[27]), was demonstrated by Demetriades and Gold,[21] Zeiberg,[35] and Pallone.[19] Others[34,36,37] have indicated a dependence on M_∞ for cones, but for cones this is essentially M_e. A correlation on M_∞ does not characterize the essence of the problem in the local wake flow field. Hence, it does not correlate both spheres and cones where the local M_e is quite different for the two geometries; in the case of spheres, M_e, not being close to M_∞.

In the Near Wake region, calculations show that M_e does not vary significantly as a function of distance downstream along the wake edge, and also that the local Mach number at the shoulder of the body (see sketch in Fig. 10 for definition of $M_{shoulder}$) is close to M_e. Therefore, here, $M_{shoulder}$ is selected as a parameter related to body shape which

is sufficiently characteristic of the local hypersonic flow field in the region near the particular body. M_{sh} is high and close to M_∞ for slender cones, and is low and close to 3 for spheres.

The x_{tr} data, as determined and published by the investigators from Lincoln Laboratory,[9] Avco/RAD,[19] Naval Ordnance Laboratory,[34] and General Motors[26] are now used on a $p_\infty \cdot x_{tr}$ vs M_{sh} plot. $p_\infty \cdot x_{tr}$ represents through binary scaling the $R_{x_{tr}}$. The correlation shown in Fig. 13 is

$$p_\infty \cdot x_{tr} = 10^{(1 + .082\, M_{sh})} \quad [\text{cm Hg} \cdot \text{cm}] \tag{10}$$

This determines the constant, a function of Mach number, for the Near Wake Law of Eq. (8). It is noted that the Near Wake correlation of (10) is also good to like a factor of two. Thus, to each value of $M_{shoulder}$, one can assign a line of negative one slope on the (x_{tr}, p_∞) plot, Fig. 10.

It should be pointed out that in the Near Wake correlation, care was exercised not to use data points in the so-called "sticking" region.[26,38] There is an upstream limit of the Near Wake transition correlation where the recompression region interacts with the wake transition processes to retard further upstream motion of x_{tr} independent of further increases in pressure. This clearly is not included in an $R_{x_{tr}}$ correlation.

Now, conceptually, the (x_{tr}, p_∞) plot, Fig. 10, can be filled with a series of vertical lines assigning a $(p_\infty)_T$ for each $\sqrt{C_D A}$ and a series of negative one-slope lines assigning an $(p_\infty \cdot x_{tr})$ for each $M_{shoulder}$. What is needed finally is an interpolation curve to connect the far wake onset altitude for the $\sqrt{C_D A}$ of the body with the near wake $R_{x_{tr}}$ behavior for the M_{sh} of the body.

7. THE INTERPOLATION REGIME

In the Interpolation Regime, one traverses from the Near to Far Wake. The strong favorable pressure gradient, the strong density gradients and the effect of body shape all become less important. Thus, compressibility effects have smaller and smaller influences in this regime, and we look at the unsteady incompressible Navier-Stokes

equation for guidance. Time is nondimensionalized with the time required for the decay of the nearly-ordered wake flow down into some given spectral distribution of random small-scale turbulence, $\tau_s = x_s/U_\infty$ and x_s is the distance to a given spectral distribution of unsteadiness, here corresponding to x_{tr}. The size of the large scale eddy, which is of the order of the size of the shear layer, is taken as the characteristic length in the y-direction. These big eddies do not grow appreciably by molecular diffusion in the time required to decay through growth of instabilities. The size of the large scale is like d for blunt bodies[8] and like d/3 for slender cones.[39] The distance required for the fluctuation level to build up to a specified finite amplitude, say Δa, is taken as the characteristic length in the x-direction, and here is equivalent to x_s.

The linearized time dependent equation of motion in the x-direction is:

$$\frac{\partial u'}{\partial t} + \bar{u}\,\frac{\partial u'}{\partial x} + v'\,\frac{\partial \bar{u}}{\partial y} = \nu\left(\frac{\partial^2 u'}{\partial y^2} + \frac{\partial^2 u'}{\partial x^2}\right) \tag{11}$$

where

$$u = \bar{u} + u'$$

with the usual notation for mean velocity, $\bar{u}$, and time dependent velocity, u'. v' is of the order of u', $u' = a(x) \cdot f(t)$ and τ_s is the time required for the fluctuation level, to build up to an amplitude Δa. Substituting into Eq. (11):

$$\frac{a}{x_s/U_\infty}\left[\frac{\partial u'}{\partial t}\right]^* + U_\infty\,\frac{\Delta a}{x_s}\left[\bar{u}\,\frac{\partial u'}{\partial x}\right]^* + a\,\frac{U}{d}\left[v'\frac{\partial \bar{u}}{\partial y}\right]^* = \nu\left(\frac{a}{d^2}\left[\frac{\partial^2 u'}{\partial y^2}\right]^* + \frac{\Delta a}{x_s^2}\left[\frac{\partial^2 u'}{\partial x^2}\right]^*\right) \tag{12}$$

where $[\ ]^*$ denotes the nondimensionalized functions and their derivatives.

If the characteristic values are appropriate, the nondimensionalized functions are of order one or less and we may look for a relationship between the nondimensional parameters. Dividing by a and neglecting terms of order $\Delta a/a$ as small, there is from (12):

$$\frac{U}{x_s} C_1 + \frac{U}{d} C_2 = \frac{\nu}{d^2} C_3 \tag{13}$$

where the C's are arbitrary constants. Rearranging

$$\frac{d}{x_s} + A = B \left(\frac{1}{R_d} \right) \tag{14}$$

The constants A and B in Eq. (14) are easily determined as the two limits of x_s: for $x_s \to \infty$, $R_d \to (R_d)_T$ and for $R_d \to \infty$, $\frac{d}{x_s}$ approaches some upstream limit, say the recompression region:

$$\frac{d}{x_s} = \left(\frac{d}{x_s} \right)_\infty \left(1 - \frac{(R_d)_T}{R_d} \right) \tag{15}$$

where $\left(\frac{d}{x_s} \right)_\infty$ is the asymptotic limit of x_s as $R_d \to \infty$. This equation is the analogue to the equation first used by Rayleigh[40] for plotting not x_s/d, the distance to a particular spectral distribution of unsteadiness, but, λ_s/d, the scale of unsteadiness at a particular x as a function of R_d:

$$\frac{d}{\lambda_s} = \left(\frac{d}{\lambda_s} \right)_\infty \left(1 - \frac{(R_d)_T}{R_d} \right) \tag{16}$$

where d/λ_s is recognized as the Strouhal No., $S = \frac{d}{\lambda_s}$. This Strouhal number - Reynolds number formula (16), was successfully used to correlate hypersonic vortex shedding data[39] had been the case for the incompressible wake.[8,22,29]

Equation (15) is the form of the $(x_s/d, R_d)$ curves of Roshko given in Fig. 6 for the incompressible case. However, for the hypersonic wake, although Eq. (15) evidences the correct asymptote for $x_s \to \infty$, $R_d = (R_d)_T$; it does not possess the necessary behavior of the Near

Wake correlation for R_d increasing: $R_{x_{tr}} = C_M$, a constant dependent on Mach number. Thus, for the purpose of the hypersonic wake, Eq. (15) is modified into

$$\left(\frac{C_M}{R_{x_{tr}}}\right) = \left(1 - \frac{(R_d)_T}{R_d}\right) \tag{17}$$

or with binary scaling and with d replaced by $\sqrt{C_D A}$:

$$\left(\frac{C_M}{p_\infty x_{tr}}\right) = \left(1 - \frac{(p_\infty \sqrt{C_D A})_T}{p_\infty \sqrt{C_D A}}\right) \tag{18}$$

This relationship is now fully determinate (the a of Eq. (4) having come out to be unity) since we have determined the correlation constants: C_M as given on the right hand side of correlation (10) and the value of $(p_\infty \sqrt{C_D A})_T$ as given on the right hand side of correlation (9). Considering the data for a single body, Eq. (18) can be simplified to

$$\frac{x_{tr}}{C_M/p_{\infty_T}} = \frac{1}{p_\infty/p_{\infty_T} - 1} \tag{19}$$

The dimensional analysis above having been presented, we take the parameters of Eq. (19) as the variables of a relationship to be determined empirically by the transition data itself:

$$\eta = \frac{x_{tr}}{C_M/p_{\infty T}} \quad \text{and} \quad \rho = p_\infty/p_{\infty T} \tag{20}$$

or on a log-log plot

$$\eta' = \log \eta; \qquad \rho' = \log \rho \tag{21}$$

It is seen that the two asymptotes are correctly given:

Far Wake: $\eta' = \infty$, $\rho' = 0$: $\quad p = (p_\infty)_T$

for the correct $\sqrt{C_D A}$ of the experimental vehicle.

Near Wake: $\eta' + \rho' = 0$: $\quad p_\infty \cdot x_{tr} = C_M$

the correct C_M corresponding to M_{sh} of the experimental vehicle. Thus,

the experimental data correlated on the variables η' and ρ' will determine a single normalized interpolation curve for all intersections of the Near and Far Wake correlations. I. e., for every vehicle in every flow field each realization of the x_{tr}, p_∞ curve is characterized by one $\sqrt{C_D A}$ and one M_{sh} — Fig. 10.

The x_{tr} data in the Interpolation regime as determined and published by the investigators from Lincoln Laboratory,[9] Avco/RAD,[19] Naval Ordnance Laboratory,[34] and General Motors[26] are now used on a η', ρ' plot, Fig. 14. The reason there is so little cone data for the Interpolation regime as well as for the Far Wake, Fig. 11, is that gun launched cones fly straight and level at high pressures. There is an obvious sparsity of data for transition onset in the downstream part of the wake, which requires experiments at lower pressure. Most transition data have been collected for the Near Wake regime because cones tend to be dynamically stable at high ambient pressures and schlieren definition is good. Almost all of the published cone data are for the Near Wake transition onset, Fig. 13. In Fig. 14 these data line up along the Near Wake asymptote: $\rho' + \eta' = 0$, and are not shown.

The Interpolation regime data in Fig. 14 are used to establish an Interpolation curve to connect the Far Wake law, (7) and (9), and the Near Wake law, (8) and (10); see Fig. 10. The Interpolation curve shown in Fig. 14 is normalized for all intersections of the Far Wake correlation (on the size of vehicle, $\sqrt{C_D A}$) and the Near Wake correlation (on the shape vehicle in any flow field, M_{sh}). Thus, it is now possible to construct a singie smooth curve which includes the representation of the Far Wake correlation and the representation of the Near Wake correlation and which has a shape not too dissimilar from Eq. (19) and the form shown in Fig. 6 for Roshko's data.

Of course, we do not know what is the quantitative nature of the spectral distribution whose forward movement is being represented by these correlations. We have assumed that each time an investigator lays down a marker on the schlieren photograph for the onset of wake unsteadiness, that each event corresponds to approximately the same

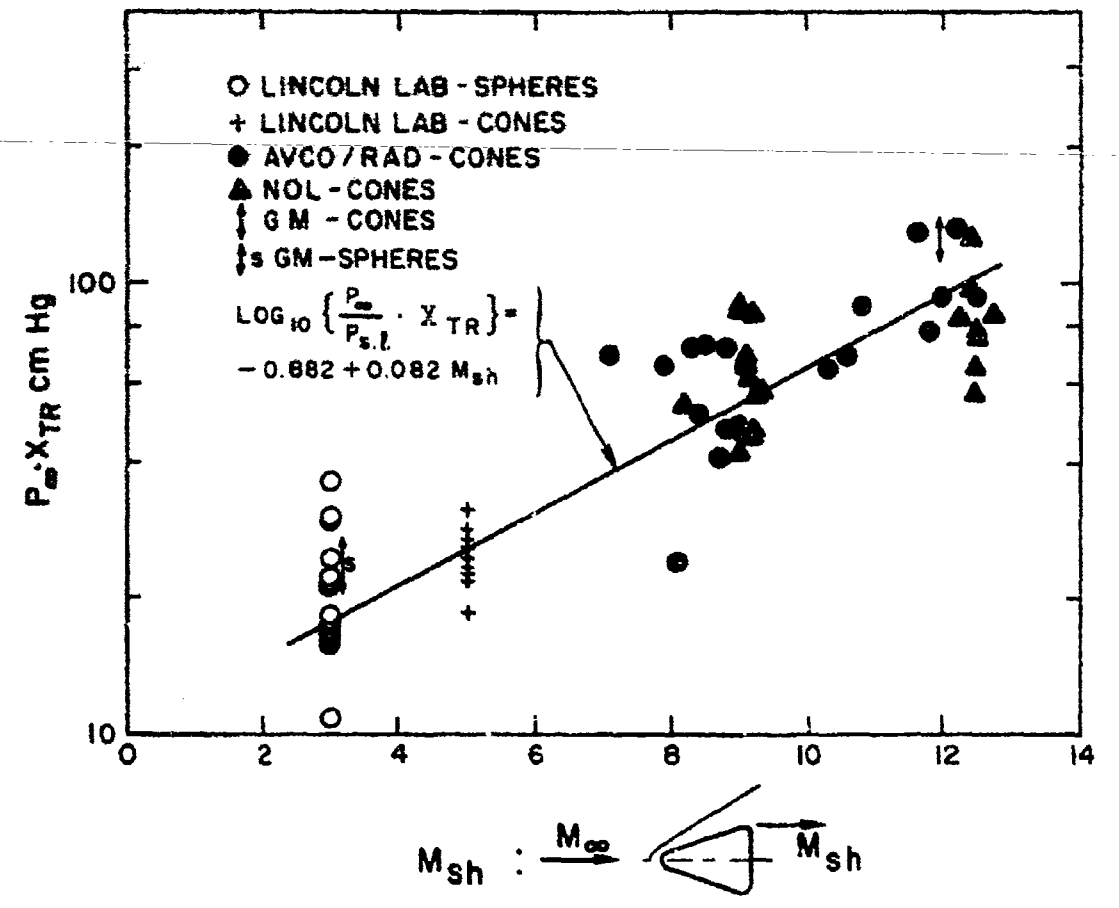

Fig. 13 Near Wake Transition Correlation. All available experimental information for air in open literature. Spheres and slender cones.

A3890

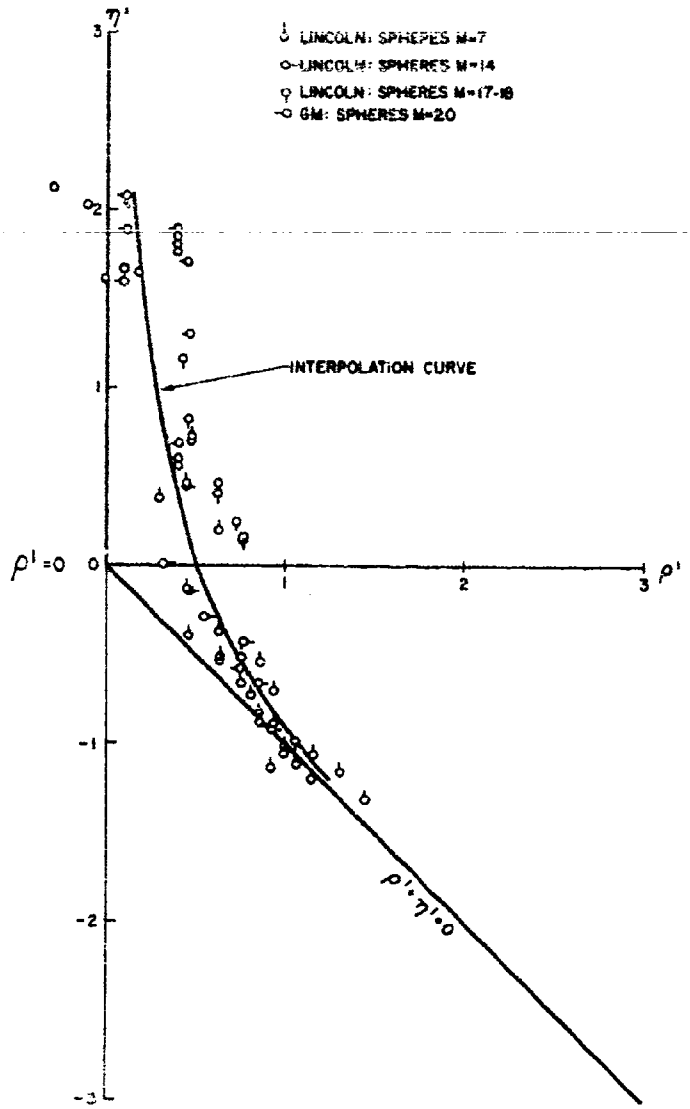

Fig. 14 The interpolation regime data correlation on $\eta' = \log x_T - \log C_M + \log (P_\infty)_T$ and $\rho' = \log P_\infty - \log (P_\infty)_T$ where the pressures have been referenced to the sea level values $P = P_\infty / P_{s.l}$ and the units of x_{tr} are feet.

spectral stimuli. Like the other correlations, the interpolation curve of Fig. 14 is good to like a factor of two.

Recently, investigations at Lincoln Laboratory[41] and General Motors[26,42] have drawn attention to phenomena which calls into question the simplicity and the smoothness of the proposed transition curve starting all the way from the Far Wake to and through the Interpolation regime into and terminating at the end of the Near Wake region, as represented in Fig. 14. To assess the nature of these considerations, we plot all of the sphere data in Fig. 15. We use the given axes in order to include data which were prosented by Slattery and Clay, only as a set of curves on this particular grid (1962, Fig. 5). Clay, Labitt and Slattery[41] claim that their high Mach number data (M_∞ = 18-20) produces a separate curve from some of their data at lower Mach number (Ref. 41, Fig. 6). However, if all of their lower Mach number data and if all of the General Motors data is included in Fig. 15, there does not show two or several separate curves but just one smooth, broad bandof data, with spread like a factor of two, with shape represented by the Near-Interpolation-Far Wake curve as developed in the present paper. In fact, it was identically these data which were used to establish the correlations developed herein.

Clay, Labitt and Slattery[41] call attention to a second feature of their data. When they consider their high speed data alone, there appears to be a sharp break to the left at about 2000 ball diameters. Wilson[26] believes his data also evidence such behavior (1965, Fig. 7). However, we see in Fig. 15 that when we place all of the sphere data on one grid, all that remains is a smooth band of data following the behavior of the correlations and interpolation developed here. As more and more data are collected, one would expect this band to become solid with data points.

A third effect was noticed by Wilson (1965)[26] for very high Mach number tests, $M_\infty \geq 20$. For blunt bodies at high Mach numbers, there is a region of high entropy production across the nearly normal part of the shock, Fig. 7. This region called the entropy wake is one of high thermal excitation and resulting low density. The sensitivity of

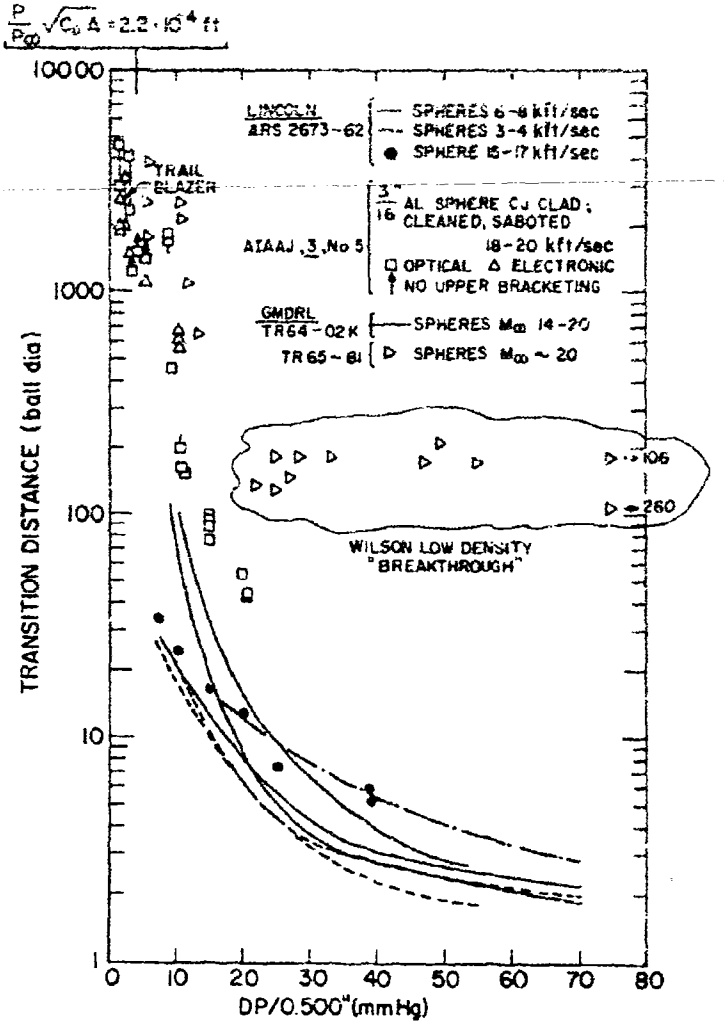

Fig. 15 All ballistic Range Sphere Transition Data.

A5272

schlieren systems is proportional to the density; and as a consequence, when the entropy wake is hot enough, as it is at very high $M_\infty \gtrsim 20$, then it becomes "opaque" to the schlieren diagnostic and shields the turbulence in the BLiW from schlieren observation. Under these experimental conditions – blunt bodies at high Mach number with a schlieren diagnostic – the turbulent BLiW would not become apparent until it had "broken through" the low density entropy regime of the SiW. Thus, even though the x_{tr} had moved upstream in the BLiW, the shielding of the schlieren diagnostic by the entropy wake would make the x_{tr} apparently remain fixed at the point where BLiW entered the high entropy region. Wilson's "break-through" data in Fig. 15 illustrates this phenomenon. However, it is important to realize that this phenomenon is clearly understandable in terms of the shielding of the BLiW by the SiW which hides from the observer the continuing forward motion of fluid mechanical transition.

8. THE HYPERSONIC WAKE TRANSITION MAP

We now construct quantitatively the hypersonic wake transition map which was shown schematically in Fig. 10. The transition map will provide a method for making the transition curve, x_{tr}, as a function of pressure ratio (altitude), for a given body size – $\sqrt{C_D A}$, and a given body shape at a given flight velocity – M_{sh}.

The Far Wake transition law was determined to be

$$\frac{p_\infty}{p_{sf}} \sqrt{C_D A} = 2.2 \times 10^{-4} \text{ ft} \qquad (9)$$

Then, to each altitude, there will correspond a body size, $\sqrt{C_D A}$, from Eq. (9), such that the wake of that body when travelling at hypersonic speeds down through that altitude will go unsteady. On the Altitude–x_{tr} Map of Fig. 10, this is represented as a vertical line at each altitude coming down from $x_{tr} \longrightarrow \infty$ for the appropriate $\sqrt{C_D A}$. This has been done in Fig. 16.

The Near Wake transition law was determined to be

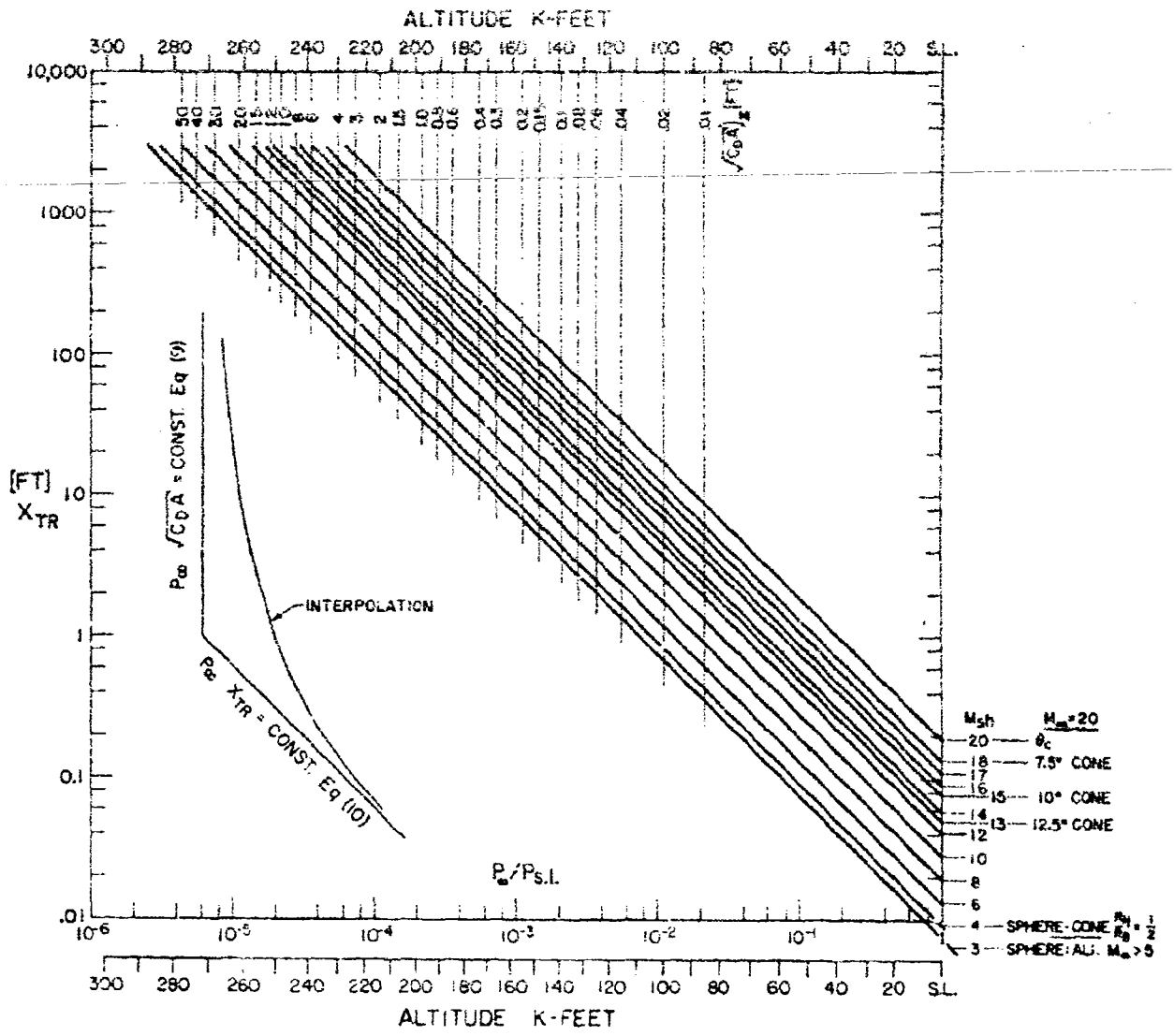

Fig. 16 Hypersonic Wake Transition Map.

A3636

$$\log_{10}\left\{\frac{p_\infty}{p_{s\ell}}\ x_{tr}\right\} = -0.882 + 0.082\, M_{sh} \qquad (10)$$

where x_{tr} is in centimeters. Hence, on the (p_∞, x_{tr}) Map of Fig. 16 there are a series of negative one-slope lines, each for a different M_{sh}. To facilitate the use of the Transition Map, there is given a conversion chart and graph for M_∞ to M_{sh}, Fig. 17.

The Interpolation curve developed in the previous section, Fig. 14, is also shown in the map, Fig. 16. For ease of use, the Interpolation curve is included with this report as a clear plastic overlay.

9. CONCLUSIONS

The Transition Map, Fig. 16, provides a method for making the transition curve, x_{tr}, as function of pressure ratio (altitude), for any given body at any given flight velocity: Connect the Far Wake onset altitude for the $\sqrt{C_D A}$ of the body with the Near Wake, $p_\infty \cdot x_{tr}$, behavior for the corresponding M_{sh} of the body. Thus, Fig. 16 becomes something of a complete Wake Transition Map for a large range of Mach numbers and body sizes and body shapes.

This map is based on an analysis which takes the Reynolds number as the correlating parameter and divides the wake transition into three regions: 1) Far Wake, where details of body shape have diffused away and the characteristic length is the total $\sqrt{C_D A}$ of the vehicle; 2) Near Wake, where local hypersonic phenomena depending on body shape dominate the flow field making it necessary to include M_{sh} in the correlation, and the characteristic length is x_{tr}; and 3) Interpolation regime, where nondimensionalization of the time dependent Navier-Stokes equation leads to the normalizing variables, $x_{tr}/(C_M/p_{\infty T})$ and $p_\infty/p_{\infty T}$, which allow a single correlation of the interpolation region data.

Only in a vehicle reentry from outside the atmosphere down to sea level can one take a single vehicle, make a single test, and with radar follow the upstream motion of x_{tr} as a function of pressure ratio (altitude). Such information is presently unavailable in the open literature and so no comparison can be made of the Map predictions with an appropriate experiment

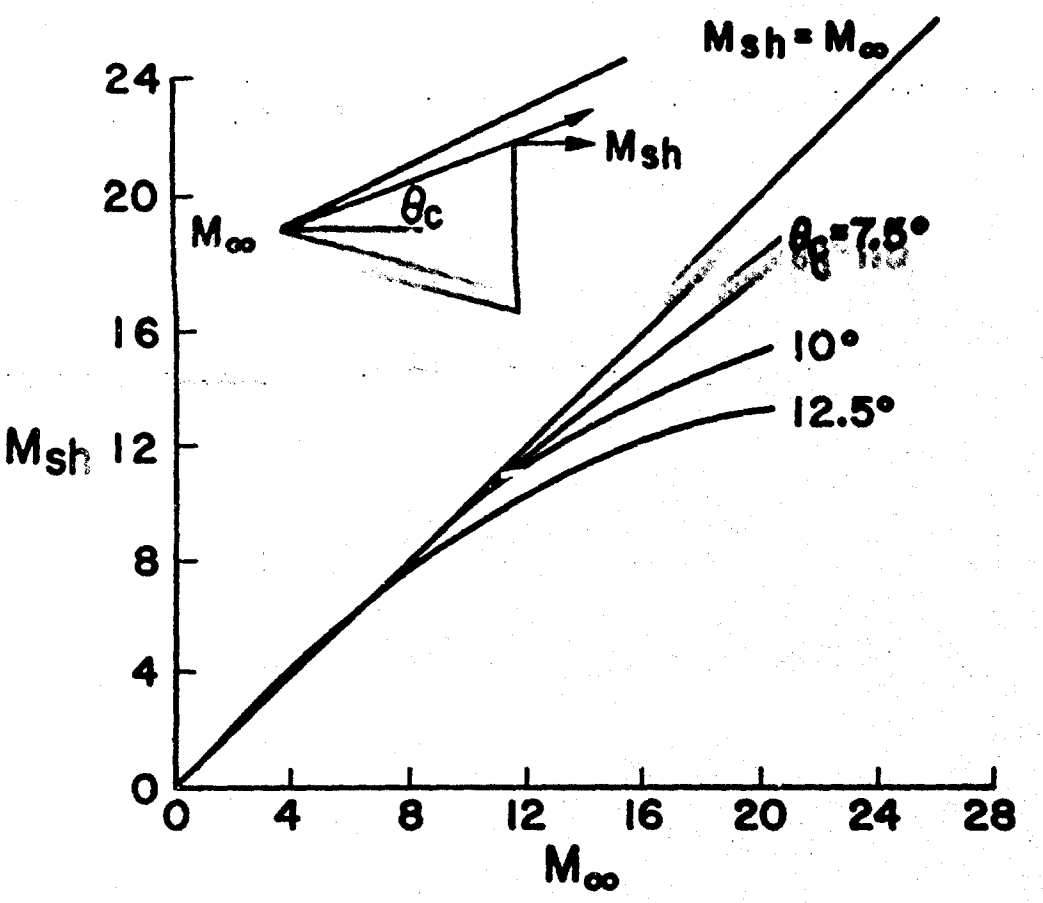

Fig. 17 M_{sh} Chart for Transition Map.

A3638

to give x_{tr} as a function of altitude for a single realization of the wake of a single vehicle. The comparison of the Map predictions with ballistic range data will be good to a factor of two because all ballistic range data available to date was used to derive the correlations, good to a factor of two, which then were used to construct the Map itself. Hence, the Map certainly applies for predicting future ballistic range results. In ballistic ranges, each firing in a given ambient gas produces one value of x_{tr} and this value will be predicted by the Map to within a factor of two.

It must be remembered that predictions based on the Transition Map are for fluid mechanical unsteadiness for a nonablating body. This fluid mechanical unsteadiness is observed by visual analysis of schlieren and shadowgraph photographs. Microwave data are for electron wake unsteadiness. It is most likely that fluid mechanical unsteadiness is a prerequisite for electron wake unsteadiness. Thus, it is to be expected that the Map predictions are closer to the body than microwave data will indicate, Fig. 5. Further, the selected location of the beginning of fluid mechanical unsteadiness as determined from visual examination of photographs is not sensitive to the wave length of the unsteadiness at that point. However, the location of wake unsteadiness as determined by microwave scattering is very sensitive to the scale of the electron unsteadiness. The wake after having gone fluid mechanically unsteady may not produce the resonant electron fluctuation scale for microwave scattering until further downstream or until a higher ambient pressure is reached. Thus, at a given pressure, the relative location of the radar wake transition further downstream than the fluid mechanical prediction is a reasonable state of affairs, even without considering the problem of electron production.

The work here for the hypersonic wake transition map has been done in the context of low or vanishingly small mass transfer from the body into the wake. The expectation in the case of high ablation mass transfer to the wake would be the following for each respective transition wake regime: 1) Far Wake: To total $\sqrt{C_D A}$, add some length characterizing the rate of momentum interchange between the ablation

products and the air encountered;[32] 2) Near Wake: Adjust M_{sh} for increased thickness of boundary layer, thus decreasing $M_{shoulder}$ and moving the transition distance forward.[26]

Finally, as the precision of the diagnostics improve and as the depth of understanding increases it is expected that modifications in detail will be necessary for the results presented here. For example, it is likely that the Near Wake transition behavior is related at a secondary level to the width of the wake. Not solely dependent on distance from the body as represented in the Near Wake correlation of Eq. (10). Waldbusser[43] and Bailey[44] will shortly demonstrate that some reduction in the spread of the data for the Near Wake correlation, Fig. 13, can be achieved by using $p_\infty \cdot x_{tr} \cdot \delta/d$ as the ordinate, where δ is the wake thickness, instead of just $p_\infty \cdot x_{tr}$ alone.

ACKNOWLEDGMENT

This analysis could only have been completed with the cooperation of those experimentalist whose data I have used. I want to express to them — Hidalgo and Taylor, Slattery and Clay, Demitriades and Gold, Kendall, Eckerman, Primich and Wilson, Lyons and Levensteins — my deep appreciation not only for the courtesy of their sharing their data with me but also for the many hours of their time which they spent on my behalf discussing their work with me.

REFERENCES

1. Landau, L. D. and Lifschitz, E. M., Fluid Mechanics, New York: Wiley (1960), Chp. III.

2. Kovaznay, L. S. G., "Hot Wire Investigation of Wake behind Cylinders at Low Reynolds Numbers," Proc. Roy. Soc. London, 198: 174-190, 1949.

3. Sato, H., "Experimental Investigation of the Transition of Laminar Separated Layer," J. of the Phys. Soc. Japan, 11, 702-709 (1956).

4. Sato, H., "The Stability and Transition of a Two-Dimensional Jet," J. Fl. Mech., 7, 53-81 (1960).

5. Sato, H. and Kuriki, K., "The Mechanism of Transition in the Wake of a Thin Flat Plate placed Parallel to a Uniform Flow," J. Fl. Mech., 11, 320-352 (1961).

6. Leonard, D. A. and Keck, J. C., "Schlieren Photography of Projectile Wakes using Resonance Radiation," ARS Jour. 32: 1112 (July 1962).

7. Goldburg, A. and Fay, J. A., "Vortex Loops in the Trails behind Hypervelocity Pellets," ARS Jour., 32: 1282 (August 1962).

8. Fay, J. A. and Goldburg, A., "Unsteady Hypersonic Wake behind Blunt Bodies," AIAA Jour., 1, 2264-2272 (1963).

9. Slattery, R. E. and Clay, W. G., "The Turbulent Wake of Hypersonic Bodies," ARS preprint 2673-62; "Experimental Measurements of Turbulent Transition Motion, Statistics and Gross Radial Growth behind Hypervelocity Objects," Phys. Fl. 5; 849-855 (1962); "Laminar-Turbulent Transition and Subsequent Motion behind Hypervelocity Spheres," ARS Jour. 32, 1427-1429 (1962).

10. Washburn, W. K. and Keck, J. C., "Racetrack Flow Visualization of Hypersonic Wakes," ARS Jour. 32: 1280 (August 1962).

11. Primich, R. I. and Steinberg, M., "A Broad Survey of Free Flight Range Measurements in the Flow about Spheres and Cones," (AMRAC IX) General Motors Defense Research Laboratory (1963 unpublished).

12. Tollmein, W., "Ein allgemeines Kriterium der Instabilitat laminarer Geschwindig keitsverteilungen," Nachr. Ges. Wiss. Gottingen Math. Phys. Klasse, Fac gruppe, I, 1, 79 (1935); NACA TM 792 (1936).

13. Pretsch, J., "Die Anfachung instabiler Storungen in einer laminaren Reibungsachicht," Jb.d. dt. Luft fahrt forschung, I. 54 (1942); NACA TM 1343 (1952).

14. Gold, H., "Hypersonic Wake Transition," Ph.D. Thesis, C.I.T., September 1963; "Stability of Axisymmetric Laminar Wakes," Proc. AIAA Entry Technology Conference, Williamsburg, Va., October 1964, pp 195-208; "Stability of Laminar Boundary Layers and Wakes at Hypersonic Speeds," (with L. Lees), Proc. International Symposium on Fundamental Phenomena in Hypersonic Flows, Buffalo, June 1964, Cornell University Press, (1966); "Laminar Stability and Laminar Turbulent Transition in Hypersonic Wakes," Avco/RAD TM-65-2 (1965).

15. Lukasiewicz, J., "Hypersonic Flow Blast Analogy," AEDC TR 61-4, (June 1961).

16. Lees, L. and Lin, C.C., "Investigation of the Stability of a Laminar Boundary Layer in a Compressible Fluid," NACA TN 1115 (1946); Lees, L., "Stability of the Laminar Boundary Layer in a Compressible Fluid," NACA TR 876 (1947).

17. Lin, C.C., "On the Stability of the Laminar Mixing Region between Two Parallel Streams in a Gas," NACA TN 2887 (1953).

18. Mack, L., "The Inviscid Stability of the Compressible Laminar Boundary Layer," JPL Space Program Summary 37-26, Vol. IV.

19. Pallone, A.J., Erdos, J.I., Eckerman, J., McKay, W., "Hypersonic Laminar Wakes and Transition Studies," AIAA Jour., 2, 855-863 (1964).

20. Primich, R.I., Robillard, P.E., Hayami, R.A., Wilson, L., and Zivanovic, S., "Radar Scattering from Wakes," General Motors Defense Research Laboratory, TR 65-01E (March 1965).

21. Demetriades, A. and Gold, H., "Correlation of Blunt-Bluff Body Wake Transition Data," GALCIT Hypersonic Research Project Memo 12, September 1962; also Demetriades, A., "Some Hot Wire Measurements in a Hypersonic Wake," Fluid Mechanics Heat Transfer Institute, 1-9 (Stanford University Press, 1961); and "Hot Wire Measurements in the Hypersonic Wakes of Slender Bodies," AIAA Preprint 63-444 (1963).

22. Roshko, A., "On the Development of Turbulent Wakes from Vortex Streets," NACA Rept. 1191 (1954).

23. Kendall, J.M., Jr., "Experimental Study of Cylinder and Sphere Wakes at a Mach Number of 3.7," California Institute of Technology, Jet Propulsion Laboratory TR 32-363 (November 1962).

24. Schlichting, H., Boundary Layer Theory, McGraw-Hill (1955), New York.

25. Goldstein, S., Modern Developments in Fluid Dynamics, Oxford University Press, Oxford (1938).

26. Wilson, L.N., "The Far Wake Behavior of Hypersonic Spheres," The General Motors Defense Research Laboratories, TR66-19, June, 1966, Wilson, L.N., "Wake Detachment Distances behind Blunt Bodies," General Motors Defense Research Laboratory (1965), Technical Report (to be published), also Wilson, L.N., "Body Shape Effects on Axisymmetric Wakes," General Motors Defense Research Laboratory, TR64-02K (October 1964).

27. Hidalgo, H., Taylor, R.L. and Keck, J.C., "Transition from Laminar to Turbulent Flow in the Viscous Wake of Blunt Bodies Flying at Hypersonic Mach Numbers," Avco Everett Research Laboratory Research Note 218 (May 1961); also, "Transition in the Viscous Wake of Blunt Bodies at Hypersonic Speeds," J. Aero. Sci., 29, 1306-1316 (November 1962).

28. Weiss, R.F. and Weinbaum, S., "Hypersonic Boundary Layer Separation and The Base Flow Problem," AIAA Jour., Vol. 4, No. 8, pp. 1321-1330 (August 1966).

29. Goldburg, A. and Florsheim, B.H., "Transition and Strouhal Number for the Incompressible Wake of Various Bodies," Phys. Fl., 9, 45-50 (1966).

30. Arkhipov, V.N., "The Formation of Streaming Fluctuations behind a Solid Object," Dokl. Abad. Nauk SSSR, 123, 53ff (1958). (English Transl.: Soviet Phys. - Doklady, 3, 1117 (1958).

31. Taneda, S., "Oscillation of the Wake behind a Flat Plate Parallel to the Flow," J. Phy. Soc. Japan, 13, 418-425 (April 1958).

32. Hunter, H.E., Private Communication.

33. Rose, P.H., Adams, M.C., Probstein, R.F., "Turbulent Heat Transfer on Highly Cooled Blunt Bodies," Heat Transfer Fluid Mechanics Inst. Proceedings, Stanford University Press, 1958, pp 143-155.

34. Lyons, W.C., Jr., Brady, J.J., and Levensteins, Z.J., "Hypersonic Drag, Stability and Wake Data for Cones and Spheres," AIAA Jour., 2, 1948-1956 (1964).

35. Zeiberg, S.L., "Transition Correlations for Hypersonic Wakes," AIAA Jour., 2, 564-565 (1964).

36. Wen, K.S., "Wake Transition," AIAA Jour. 2, 956-957 (1964).

37. Waldbusser, E., "The Relationship of Laminar Wake Width to Wake Transition Distance," AIAA Jour. 3, 1965-1966 (1965).

38. Webb, W. H., Hromas, L. and Lees, L., "Hypersonic Wake Transition," AIAA Jour., 1, 719-721 (1963).

39. Goldburg, A., Washburn, W.K. and Florsheim, B.H., "Strouhal Numbers for the Hypersonic Wakes of Spheres and Cones," AIAA Jour. 3, 1332-1333 (1965).

40. Rayleigh, L., Phil. Mag., 29, 433-453 (1915).

41. Clay, W.G., Labitt, M. and Slattery, R.E., "Measured Transition from Laminar to Turbulent Flow," AIAA Jour., 3, 837-841 (May 1965).

42. Wilson, L.N., "Detached Wakes Behind Conical Reentry Bodies", (to be published 1967).

43. Waldbusser, E., "Shape Effects on Hypersonic Slender Body Wake Geometry and Transition Distance," (to be published, AIAA J., 1967).

44. Bailey, A.B., AEDC Tech. Rept. 66-137, July 1966 (limited distribution).

Unclassified
Security Classification

DOCUMENT CONTROL DATA - R&D

(Security classification of title, body of abstract and indexing annotation must be entered when the overall report is classified)

1 ORIGINATING ACTIVITY (Corporate author)
Avco Everett Research Laboratory
2385 Revere Beach Parkway
Everett, Massachusetts

2a REPORT SECURITY CLASSIFICATION
Unclassified

2b GROUP

3 REPORT TITLE
A SUMMARY ANALYSIS OF LABORATORY HYPERSONIC WAKE TRANSITION EXPERIMENTS

4 DESCRIPTIVE NOTES (Type of report and inclusive dates)
Research Note 672

5 AUTHOR(S) (Last name, first name, initial)
Goldburg, A.

6 REPORT DATE	7a TOTAL NO. OF PAGES	7b NO. OF REFS
December 1966	58	44

8a CONTRACT OR GRANT NO
DA-01-021-AMC-12005 (Z)
(part of Project DEFENDER)
b PROJECT NO

9a ORIGINATOR'S REPORT NUMBER(S)
Research Note 672

9b OTHER REPORT NO(S) (Any other numbers that may be assigned this report)

10 AVAILABILITY/LIMITATION NOTICES
Qualified requesters may obtain copies of this report from DDC.

11 SUPPLEMENTARY NOTES

12 SPONSORING MILITARY ACTIVITY
ARPA, monitored by the Army Missile Command, United States Army Redstone Arsenal, Alabama

13 ABSTRACT

Hypersonic Wake Transition data over a range of Reynolds numbers have been obtained over the past several years at many laboratories. In the present paper, the available experimental data is structured into three laws: The Law of the Far Wake, The Law of the Near Wake, and The Law of the Interpolation Regime. These three laws are then represented on a single Hypersonic Wake Transition Map.

The Reynolds number is selected as the correlating parameter, where local conditions, characterizing the state of the gas at transition are used for the property values. The correlating constant is determined from the ballistic range data. For high Mach number flows, binary scaling allows the representation of the Reynolds number as a pressure times a length.

In the Far Wake, for the first onset of wake unsteadiness, the wake velocity profiles have reached their asymptotic behavior, density gradients have become small, and details of body shape have been lost. For this region, the characteristic length is represented as $\sqrt{C_D A}$ based on the total drag of the body. The Far Wake transition rule becomes $p_\infty \sqrt{C_D A}$ = constant.

In the Near Wake, local hypersonic phenomena depending on body shape dominate the flow field. Here the characteristic length is the distance from the wake origin to the onset of unsteadiness, x_{tr}. As in boundary layer flow this correlation shows a strong dependence on an appropriate local Mach number, M_e, at the point of wake transition: $p_\infty \cdot x_{tr}$ = constant a function of M_e.

In the Interpolation Regime, one traverses from the Near to the Far Wake. The stong favorable pressure gradient, the strong density gradients and the effect of body shape becomes less important as one proceeds downstream along the Wake in the Interpolation regime. Thus, ideas derived from the Navier-Stokes equation are useful and lead with the aid of the ballistic range data to a sufficiently accurate general interpolation curve to connect the Far Wake Law with the Near Wake Law. The Interpolation curve, like the $p_\infty \cdot \sqrt{C_D A}$ Far Wake and the $p_\infty \cdot x_{tr}$ Near Wake correlation is good to a factor of 2 in the pressure.

The Transition Map provides a method for making the transition curve, x_{tr} as function of pressure ratio (altitude), for a given body at a given flight velocity: Connect the Far Wake onset altitude for the $\sqrt{C_D A}$ (size) of the body with the Near Wake $Re_{x_{tr}}$ behavior for the corresponding M_{sh} (shape) of the body. Thus a complete qualitative Wake Transition Map is presented for a large range of Mach numbers and body sizes and body shapes.

*This paper is a summary of the author's work on this topic over the several years he was associated with Avco Everett Research Laboratory. It is being published at this time for the purpose of exchange and stimulation of ideas and not as an implicit approval of the findings and conclusions therein.

DD FORM 1 JAN 64 1473

Unclassified
Security Classification

KEY WORDS	LINK A		LINK B		LINK C	
	ROLE	WT	ROLE	WT	ROLE	WT
1. Wakes						
2. Hypersonic						
3. Transition						
4. Turbulence						
5. Scaling						
6. Spheres						
7. Cones						

INSTRUCTIONS

1. ORIGINATING ACTIVITY: Enter the name and address of the contractor, subcontractor, grantee, Department of Defense activity or other organization *(corporate author)* issuing the report.

2a. REPORT SECURITY CLASSIFICATION: Enter the overall security classification of the report. Indicate whether "Restricted Data" is included. Marking is to be in accordance with appropriate security regulations.

2b. GROUP: Automatic downgrading is specified in DoD Directive 5200.10 and Armed Forces Industrial Manual. Enter the group number. Also, when applicable, show that optional markings have been used for Group 3 and Group 4 as authorized.

3. REPORT TITLE: Enter the complete report title in all capital letters. Titles in all cases should be unclassified. If a meaningful title cannot be selected without classification, show title classification in all capitals in parenthesis immediately following the title.

4. DESCRIPTIVE NOTES: If appropriate, enter the type of report, e.g., interim, progress, summary, annual, or final. Give the inclusive dates when a specific reporting period is covered.

5. AUTHOR(S): Enter the name(s) of author(s) as shown on or in the report. Enter last name, first name, middle initial. If military, show rank and branch of service. The name of the principal author is an absolute minimum requirement.

6. REPORT DATE: Enter the date of the report as day, month, year, or month, year. If more than one date appears on the report, use date of publication.

7a. TOTAL NUMBER OF PAGES: The total page count should follow normal pagination procedures, i.e., enter the number of pages containing information.

7b. NUMBER OF REFERENCES: Enter the total number of references cited in the report.

8a. CONTRACT OR GRANT NUMBER: If appropriate, enter the applicable number of the contract or grant under which the report was written.

8b, 8c, & 8d. PROJECT NUMBER: Enter the appropriate military department identification, such as project number, subproject number, system numbers, task number, etc.

9a. ORIGINATOR'S REPORT NUMBER(S): Enter the official report number by which the document will be identified and controlled by the originating activity. This number must be unique to this report.

9b. OTHER REPORT NUMBER(S): If the report has been assigned any other report numbers *(either by the originator or by the sponsor)*, also enter this number(s).

10. AVAILABILITY/LIMITATION NOTICES: Enter any limitations on further dissemination of the report, other than those imposed by security classification, using standard statements such as:

(1) "Qualified requesters may obtain copies of this report from DDC."

(2) "Foreign announcement and dissemination of this report by DDC is not authorized."

(3) "U. S. Government agencies may obtain copies of this report directly from DDC. Other qualified DDC users shall request through _____."

(4) "U. S. military agencies may obtain copies of this report directly from DDC. Other qualified users shall request through _____."

(5) "All distribution of this report is controlled. Qualified DDC users shall request through _____."

If the report has been furnished to the Office of Technical Services, Department of Commerce, for sale to the public, indicate this fact and enter the price, if known.

11. SUPPLEMENTARY NOTES: Use for additional explanatory notes.

12. SPONSORING MILITARY ACTIVITY: Enter the name of the departmental project office or laboratory sponsoring *(paying for)* the research and development. Include address.

13. ABSTRACT: Enter an abstract giving a brief and factual summary of the document indicative of the report, even though it may also appear elsewhere in the body of the technical report. If additional space is required, a continuation sheet shall be attached.

It is highly desirable that the abstract of classified reports be unclassified. Each paragraph of the abstract shall end with an indication of the military security classification of the information in the paragraph, represented as *(TS), (S), (C)* or *(U)*

There is no limitation on the length of the abstract. However, the suggested length is from 150 to 225 words.

14. KEY WORDS: Key words are technically meaningful terms or short phrases that characterize a report and may be used as index entries for cataloging the report. Key words must be selected so that no security classification is required. Identifiers, such as equipment model designation, trade name, military project code name, geographic location, may be used as key words but will be followed by an indication of technical context. The assignment of links, rules, and weights is optional

Unclassified
Security Classification

DOCUMENT CONTROL DATA - R&D

(Security classification of title, body of abstract and indexing annotation must be entered when the overall report is classified)

1 ORIGINATING ACTIVITY (Corporate author)

Avco Everett Research Laboratory
2385 Revere Beach Parkway
Everett, Massachusetts

2a REPORT SECURITY CLASSIFICATION
Unclassified

2b GROUP

3 REPORT TITLE

A SUMMARY ANALYSIS OF LABORATORY HYPERSONIC WAKE TRANSITION EXPERIMENTS

4 DESCRIPTIVE NOTES (Type of report and inclusive dates)

Research Note 672

5 AUTHOR(S) (Last name, first name, initial)

Goldburg, A.

6 REPORT DATE	7a TOTAL NO OF PAGES	7b NO OF REFS
December 1966	58	44

8a CONTRACT OR GRANT NO	9a ORIGINATOR'S REPORT NUMBER(S)
AF 04(694)-690	Research Note 672
b PROJECT NO	9b OTHER REPORT NO(S) (Any other numbers that may be assigned this report)
	BSD-TR-66-375

10 AVAILABILITY LIMITATION NOTICES

This document is subject to special export controls and each transmittal to foreign governments or foreign nationals may be made only with prior approval of: Ballistic Systems Division (BSYDV) Norton AFB, Calif. 92409.

11 SUPPLEMENTARY NOTES	12 SPONSORING MILITARY ACTIVITY
	BSD-Deputy for Ballistic Missile Re-entry Systems AFSC, Norton AFB, CAlifornia

13 ABSTRACT

Hypersonic Wake Transition data over a range of Reynolds numbers have been obtained over the past several years at many laboratories. In the present paper, the available experimental data is structured into three laws: The Law of the Far Wake, The Law of the Near Wake, and The Law of the Interpolation Regime. These three laws are then represented on a single Hypersonic Wake Transition Map.

The Reynolds number is selected as the correlating parameter, where local conditions, characterizing the state of the gas at transition are used for the property values. The correlating constant is determined from the ballistic range data. For high Mach number flows, binary scaling allows the representation of the Reynolds number as a pressure times a length.

In the Far Wake, for the first onset of wake unsteadiness, the wake velocity profiles have reached their asymptotic behavior, density gradients have become small, and details of body shape have been lost. For this region, the characteristic length is represented as $\sqrt{C_D A}$ based on the total drag of the body. The Far Wake transition rule becomes $p_\infty \cdot \sqrt{C_D A} = \text{constant}$.

In the Near Wake, local hypersonic phenomena depending on body shape dominate the flow field. Here the characteristic length is the distance from the wake origin to the onset of unsteadiness, x_{tr}. As in boundary layer flow this correlation shows a strong dependence on an appropriate local Mach number, M_e, at the point of wake transition: $p_\infty \cdot x_{tr} = \text{constant}$, a function of M_e.

In the Interpolation Regime, one traverses from the Near to the Far Wake. The strong favorable pressure gradient, the strong density gradients and the effect of body shape becomes less important as one proceeds downstream along the Wake in the Interpolation regime. Thus, ideas derived from the Navier-Stokes equation are useful and lead with the aid of the ballistic range data to a sufficiently accurate general interpolation curve to connect the Far Wake Law with the Near Wake Law. The Interpolation curve, like the $p_\infty \cdot \sqrt{C_D A}$ Far Wake and the $p_\infty \cdot x_{tr}$ Near Wake correlation is good to a factor of 2 in the pressure.

The Transition Map provides a method for making the transition curve, x_{tr} as function of pressure ratio (altitude), for a given body at a given flight velocity: Connect the Far Wake onset altitude for the $\sqrt{C_D A}$ (size) of the body with the Near Wake $Re_{x_{tr}}$ behavior for the corresponding M_{sh} (shape) of the body. Thus a complete qualitative Wake Transition Map is presented for a large range of Mach numbers and body sizes and body shapes.

*This paper is a summary of the author's work on this topic over the several years he was associated with Avco Everett Research Laboratory. It is being published at this time for the purpose of exchange and stimulation of ideas and not as an implicit approval of the findings and conclusions therein.

DD FORM 1 JAN 64 1473

Unclassified
Security Classification

KEY WORDS	LINK A		LINK B		LINK C	
	ROLE	WT	ROLE	WT	ROLE	WT
1. Wakes						
2. Hypersonic						
3. Transition						
4. Turbulence						
5. Scaling						
6. Spheres						
7. Cones						

INSTRUCTIONS

1. ORIGINATING ACTIVITY: Enter the name and address of the contractor, subcontractor, grantee, Department of Defense activity or other organization *(corporate author)* issuing the report.

2a. REPORT SECURITY CLASSIFICATION: Enter the overall security classification of the report. Indicate whether "Restricted Data" is included. Marking is to be in accordance with appropriate security regulations.

2b. GROUP: Automatic downgrading is specified in DoD Directive 5200.10 and Armed Forces Industrial Manual. Enter the group number. Also, when applicable, show that optional markings have been used for Group 3 and Group 4 as authorized.

3. REPORT TITLE: Enter the complete report title in all capital letters. Titles in all cases should be unclassified. If a meaningful title cannot be selected without classification, show title classification in all capitals in parenthesis immediately following the title.

4. DESCRIPTIVE NOTES: If appropriate, enter the type of report, e.g., interim, progress, summary, annual, or final. Give the inclusive dates when a specific reporting period is covered.

5. AUTHOR(S): Enter the name(s) of author(s) as shown on or in the report. Enter last name, first name, middle initial. If military, show rank and branch of service. The name of the principal author is an absolute minimum requirement.

6. REPORT DATE: Enter the date of the report as day, month, year, or month, year. If more than one date appears on the report, use date of publication.

7a. TOTAL NUMBER OF PAGES: The total page count should follow normal pagination procedures, i.e., enter the number of pages containing information.

7b. NUMBER OF REFERENCES: Enter the total number of references cited in the report.

8a. CONTRACT OR GRANT NUMBER: If appropriate, enter the applicable number of the contract or grant under which the report was written.

8b, 8c, & 8d. PROJECT NUMBER: Enter the appropriate military department identification, such as project number, subproject number, system numbers, task number, etc.

9a. ORIGINATOR'S REPORT NUMBER(S): Enter the official report number by which the document will be identified and controlled by the originating activity. This number must be unique to this report.

9b. OTHER REPORT NUMBER(S): If the report has been assigned any other report numbers *(either by the originator or by the sponsor)*, also enter this number(s).

10. AVAILABILITY/LIMITATION NOTICES: Enter any limitations on further dissemination of the report, other than those imposed by security classification, using standard statements such as:

(1) "Qualified requesters may obtain copies of this report from DDC."

(2) "Foreign announcement and dissemination of this report by DDC is not authorized."

(3) "U. S. Government agencies may obtain copies of this report directly from DDC. Other qualified DDC users shall request through _____."

(4) "U. S. military agencies may obtain copies of this report directly from DDC. Other qualified users shall request through _____."

(5) "All distribution of this report is controlled. Qualified DDC users shall request through _____."

If the report has been furnished to the Office of Technical Services, Department of Commerce, for sale to the public, indicate this fact and enter the price, if known.

11. SUPPLEMENTARY NOTES: Use for additional explanatory notes.

12. SPONSORING MILITARY ACTIVITY: Enter the name of the departmental project office or laboratory sponsoring *(paying for)* the research and development. Include address.

13. ABSTRACT: Enter an abstract giving a brief and factual summary of the document indicative of the report, even though it may also appear elsewhere in the body of the technical report. If additional space is required, a continuation sheet shall be attached.

It is highly desirable that the abstract of classified reports be unclassified. Each paragraph of the abstract shall end with an indication of the military security classification of the information in the paragraph, represented as *(TS), (S), (C), or (U)*.

There is no limitation on the length of the abstract. However, the suggested length is from 150 to 225 words.

14. KEY WORDS: Key words are technically meaningful terms or short phrases that characterize a report and may be used as index entries for cataloging the report. Key words must be selected so that no security classification is required. Identifiers, such as equipment model designation, trade name, military project code name, geographic location, may be used as key words but will be followed by an indication of technical context. The assignment of links, rules, and weights is optional.